Conjugation-Length Dependence of the T_1 Lifetimes of Carotenoids Free in Solution and Incorporated into the LH2, LH1, RC, and RC-LH1 Complexes: Possible Mechanisms of Triplet-Energy Dissipation†

Yoshinori Kakitani,‡ Junji Akahane,‡ Hidekazu Ishii,‡ Hiroshi Sogabe,‡ Hiroyoshi Nagae,§ and Yasushi Koyama*,‡

Faculty of Science and Technology, Kwansei Gakuin University, 2-1 Gakuen, Sanda 669-1337, Japan, and Kobe City University of Foreign Studies, Gakuen-Higashimachi, Nishi-ku, Kobe 651-2187, Japan

Received October 29, 2006; Revised Manuscript Received December 6, 2006

ABSTRACT: In addition to the roles of antioxidant and spacer, carotenoids (Cars) in purple photosynthetic bacteria pursue two physiological functions, i.e., light harvesting and photoprotection. To reveal the mechanisms of the photoprotective function, i.e., quenching triplet bacteriochlorophyll to prevent the sensitized generation of singlet oxygen, the triplet absorption spectra were recorded for Cars, where the number of conjugated double bonds (*n*) is in the region of 9−13, to determine the dependence on *n* of the triplet lifetime. The Cars examined include those in (a) solution; (b) the reconstituted LH1 complexes; (c) the native LH2 complexes from *Rba. sphaeroides* G1C, *Rba. sphaeroides* 2.4.1, *Rsp. molischianum*, and *Rps. acidophila* 10050; (d) the RCs from *Rba. sphaeroides* G1C, *Rba. sphaeroides* 2.4.1, and *Rsp. rubrum* S1; and (e) the RC-LH1 complexes from *Rba. sphaeroides* G1C, *Rba. sphaeroides* 2.4.1, *Rsp. molischianum*, *Rps. acidophila* 10050, and *Rsp. rubrum* S1. The results lead us to propose the following mechanisms: (i) A substantial shift of the linear dependence to shorter lifetimes on going from solution to the LH2 complex was ascribed to the twisting of the Car conjugated chain. (ii) A substantial decrease in the slope of the linear dependence on going from the reconstituted LH1 to the LH1 component of the RC-LH1 complex was ascribed to the minor-component Car forming a leak channel of triplet energy. (iii) The loss of conjugation-length dependence on going from the isolated RC to the RC component of the RC-LH1 complex was ascribed to the presence of a triplet-energy reservoir consisting of bacteriochlorophylls in the RC component.

The photosynthetic unit in purple photosynthetic bacteria consists of the reaction center (RC),[1] the surrounding central light-harvesting complex (LH1), and the peripheral light-harvesting complex (LH2) (*1*). Some strains have the LH2 complex, but others do not. The detailed structures have been determined, by X-ray crystallography, for the RCs from *Rhodopseudomonas* (*Rps.*) *viridis* (*2*) and *Rhodobacter* (*Rba.*) *sphaeroides* (*3*) as well as for the LH2 complexes from *Rps. acidophila* (*4*) and *Rhodospirillum* (*Rsp.*) *molischianum* (*5*). A first structure of the RC-LH1 complex has been reported recently (*6*). This particular complex consists of the RC component and the LH1 component containing 15 subunits and a peptide called pufX. One carotenoid (Car), two bacteriochlorophylls (BChls), and α- and *β*-peptides form the subunit.

Cars constitute one of the most diverse families of multipurpose organic molecules, whose respective roles in photosynthetic and nonphotosynthetic organisms still remain unclear. In addition to the roles of antioxidant and spacer, Cars in purple photosynthetic bacteria pursue two physiological functions, i.e., light harvesting and photoprotection (*7*, *8*). In the former, Car harvests the light energy and transfers its singlet energy to BChl, whereas in the latter, Car quenches the lowest-triplet (T_1) state of special-pair BChls (^{3}P) that is generated by reverse electron transfer followed by charge recombination and dissipates the transferred triplet energy as heat.

In relation to these functions, the natural selection of the Car configurations, i.e., the all-*trans* configuration by both LH complexes and the 15-*cis* configuration by the RC, has been found (see ref *9* for a review). Furthermore, our recent analysis of Cars in *Rubrivivax* (*Rvi.*) *gelatinosus*, having both the spheroidene and the spirilloxanthin biosynthetic pathways, showed that Cars having a shorter conjugated chain are selectively bound to the LH2 complex, whereas Cars having a longer conjugated chain are selectively bound to the RC (Kakitani et al. Unpublished results). The reason for

† This work has been supported by a grant, Open Research Center Project (Research Center of Photo-Energy Conversion) from the Ministry of Education, Culture, Sports, Science and Technology, Japan. Y. Kakitani has been supported by Research Fellowships of the Japan Society for the Promotion of Science for Young Scientists.

* To whom correspondence should be addressed. Tel/Fax: +81-79-565-8408. E-mail: ykoyama@kwansei.ac.jp.

‡ Kwansei Gakuin University.

§ Kobe City University of Foreign Studies.

[1] Abbreviations; BChl, bacteriochlorophyll; Car, carotenoid; HPLC, high-pressure liquid chromatography; ISC, intersystem crossing; LDAO, *N*,*N*-dimethyldodecylamine-*N*-oxide; LH, light-harvesting complex; *n*, the number of conjugated double bonds; OTG, *n*-octyl-*β*-D-thioglucopyranoside; P, special-pair bacteriochlorophyll; $P^{+\bullet}$, special-pair radical cation; *Rba.*, *Rhodobacter*; RC, reaction center; *Rps.*, *Rhodopseudomonas*; *Rsp.*, *Rhodospirillum*; *Rvi.*, *Rubrivivax*; S_0, the ground state; SADS, species-associated difference spectra; SC, sodium cholate; SVD, singular-value decomposition; T_1, the lowest triplet state.

10.1021/bi062237z CCC: $37.00
Published on Web 01/31/2007

Table 1: Car Compositions (in %) in the LH2, RC, and RC-LH1 Complexes[a,b]

Cars[c]	*Rba. sphaeroides* G1C	*Rba. sphaeroides* 2.4.1	*Rsp. molischianum*	*Rps. acidophila* 10050	*Rsp. rubrum* S1
		(a) LH2			
neu ($n = 9$)	93	11			
sph ($n = 10$)	7	89			
lyc ($n = 11$)			14	20	
rhd ($n = 11$)			86		
rhd-g ($n = 11$)				80	
		(b) RC			
neu ($n = 9$)	100				
sph ($n = 10$)		100			
anh ($n = 12$)					6
spx ($n = 13$)					94
		(c) RC-LH1			
neu ($n = 9$)	93	9			
sph ($n = 10$)		85			
lyc ($n = 11$)	7		40	21	
rhd ($n = 11$)			60		
rhd-g ($n = 11$)				17	
anh ($n = 12$)				15	6
rhv ($n = 12$)					4
spx ($n = 13$)		6		47	90

[a] The extinction coefficient (ϵ) determined for neurosporene ($n = 9$), spheroidene ($n = 10$), lycopene ($n = 11$), anhydrorhodovibrin ($n = 12$), and spirilloxanthin ($n = 13$) are transferred to other Cars having the same n. [b] Components not larger than 4% are excluded. [c] Abbreviations: neu, neurosporene; sph, spheroidene; lyc, lycopene; rhd, rhodopin; rhd-g, rhodopin glucoside; anh, anhydrorhodovibrin; rhv, rhodovibrin; and spx, spirilloxanthin.

the structural selection of the conjugated chain, i.e., (i) the all-*trans* shorter conjugated chain by the LH complexes and (ii) the 15-*cis* longer conjugated chain by the RC, can now be explained as follows (see refs *8* and *10* for reviews).

(i) The all-*trans* conjugated chain has approximate C_{2h} symmetry, which gives rise to low-lying singlet states with different symmetries that are energetically located closeby. Then, these singlet states of Car can facilitate multichannel singlet energy-transfer pathways to the Q_x and Q_y states of BChl, during the processes of stepwise singlet internal conversion. All of those singlet states decrease in energy with the number of conjugated double bonds, n, as linear functions of $1/(2n + 1)$ (*11*) as in the case of polyenes (*12*, *13*). Therefore, Cars having a shorter conjugated chain ($n = 9$ and 10) and, as a result, a higher singlet energy, are advantageous for singlet-energy transfer to BChl (see, for reviews, refs *14* and *15*).

(ii) 15-*cis* Cars in solution most efficiently isomerize into all-*trans* upon triplet excitation (see ref *16* for a review). This rotational motion toward all-*trans*, in the binding pocket of the RC, causes a change in the orbital angular momentum and, through the spin−orbit coupling, a change in the spin angular momentum, which results in the T_1 (the lowest triplet state) $\rightarrow$ S_0 (the ground state) intersystem crossing (ISC) dissipating the T_1 energy (*17*, *18*). The T_1 energy also lowers with n (*12*, *13*, *19*); therefore, Cars having a longer conjugated chain and, as a result, a lower energy, are advantageous for accepting triplet energy from BChl and for dissipation.

We found that the RCs from *Rba. sphaeroides* G1C, *Rba. sphaeroides* 2.4.1, and *Rsp. rubrum* S1 contain neurosporene ($n = 9$), spheroidene ($n = 10$), and spirilloxanthin ($n = 13$) as the major components, respectively (see Table 1b). All three strains grow equally well under similar light conditions. Then, a question arises; how can they subsidize the advantage/disadvantage in the light-harvesting and photoprotective functions of Cars mentioned above, assuming that the assemblies and functions of BChls and peptides are very similar to one another? There must be some mechanism to balance the incoming singlet energy and the outgoing triplet energy. The mechanism must enhance the dissipation of the triplet energy in strains with a shorter chain Car that is more efficient in the light-harvesting function, whereas it must suppress the triplet-energy dissipation in the strain with a longer chain Car that is less efficient in the light-harvesting function. In addition, the LH1 components of the RC-LH1 complexes from the above strains additionally contain, as minor-component Cars, lycopene ($n = 11$), neurosporene ($n = 9$) + spirilloxanthin ($n = 13$), and anhydrorhodovibrin + rhodovibrin (both $n = 12$), respectively (Table 1c). The minor-component Cars may play a role in the triplet-energy dissipation.

The triplet-state Cars (^{3}Cars) in the RC have been extensively studied concerning (i) the mechanism of triplet generation (*20*−*23*) and (ii) triplet-energy transfer from the special-pair BChls (P; *24*−*30*). On the other hand, the ^{3}Cars in the LH complexes and membranes have been studied less extensively, concerning (i) the mechanisms of triplet generation (*31*−*35*) and (ii) triplet-energy transfer from the triplet-state BChl (^{3}BChl; *36*−*39*).

Most recently, Feng et al. (*40*) examined, by time-resolved absorption spectroscopy, ^{3}Cars in the LH2 complex from *Rps. palustris*. The authors found, following pulsed excitation of BChl, rapid spectral changes in the $T_n \leftarrow T_1$ absorption of Cars (in the 0.6−1.0 μs time range). They ascribed this observation to an equilibration dynamics among Cars having various conjugation lengths. The triplet-energy transfer between a pair of Cars may be relevant to the role of the minor-component Cars mentioned above.

On the other hand, Alric (*41*) examined, by the same method, the LH2 and RC-LH1 complexes as well as the membranes and cells of *Rvi. gelatinosus*. Taking advantage of the unique characteristics of this bacterium, the authors elegantly succeeded in separately probing the T_1 states of LH2-bound spheroidene and the RC-bound spirilloxanthin. He found, under reducing conditions, that the excess light energy was first dissipated by the formation of T_1 spirilloxanthin in the RC, and a further increase of light energy enhanced the formation of T_1 spheroidene in the antenna complex. Under the oxidizing conditions, only the spheroidene triplet was formed. This redox dependence of triplet generation may be relevant to the mechanism of triplet-energy dissipation in the higher order assembly of a pigment−protein complex such as the RC-LH1 complex.

Stimulated by the above interesting observations, we have focused our attention, in the present investigation, on the conjugation-length (n) dependence of the T_1 lifetimes in Cars in solution and in the LH1, LH2, RC, and RC-LH1 complexes and have addressed the following three specific questions.

Question 1: How can the intermolecular interaction in the LH complexes, among Car, BChl, and peptides, affect the triplet-energy dissipation? Can this interaction affect the conjugation-length dependence of the T_1 lifetime?

Question 2: What is the function of the minor-component Cars in the LH1 component of the RC-LH1 complex? Can they subsidize the conjugation-length dependence of triplet-energy dissipation?

Question 3: How can the intercomplex interaction, between the RC and the LH1 components in the RC-LH1 complex, affect the triplet-energy dissipation? Can the interaction subsidize the conjugation-length dependence of triplet-energy dissipation?

We hope that the usage of a set of Cars with different conjugation lengths in each pigment−protein complex will provide more reliable pieces of information.

MATERIALS AND METHODS

Preparation of Samples. (a) Cars were isolated by the methods described previously: neurosporene ($n = 9$) and spheroidene ($n = 10$) from *Rba. sphaeroides* G1C and 2.4.1, respectively (*42*), lycopene ($n = 11$) from tomato juice (*43*), anhydrorhodovibrin ($n = 12$) from *Chromatium vinosum* (*44*), and spirilloxanthin ($n = 13$) from *Rsp. rubrum* S1 (*11*). The sensitizer, BChl *a*, was isolated as described previously (*45*).

(b) The LH2 complexes containing Cars ($n = 9$, 10, 11, and 11) were isolated, as described previously, from *Rba. sphaeroides* G1C and *Rba. sphaeroides* 2.4.1 (*46*, *47*), *Rsp. molischianum* (*48*), and *Rps. acidophila* 10050 (*49*).

(c) The preparation of reconstituted LH1, i.e., incorporating one of the Cars ($n = 9-13$), i.e., neurosporene, spheroidene, lycopene, anhydrorhodovibrin, or spirilloxanthin, into the LH1 complex from *Rsp. rubrum* G9 was described previously (*50*, *51*). In the present reconstitution, Cars with the methoxy group, i.e., methoxyneurosporene ($n = 9$) and tetrahydrospirilloxanthin ($n = 11$), were used instead of neurosporene and lycopene. Those Cars were isolated from *Rba. sphaeroides* Ga in reference to the previous method (*42*). The detailed procedure is described in the Supporting Information.

(d) Those RCs containing Cars ($n = 9$, 10, and 13) were isolated from *Rba. sphaeroides* G1C, *Rba. sphaeroides* 2.4.1, and *Rsp. rubrum* S1, respectively. (i) The RCs from *Rba. sphaeroides* G1C and 2.4.1 were isolated by the method described previously (*52*) with some modification. The details are described in the Supporting Information. (ii) The RC from *Rsp. rubrum* was isolated based on the previous method (*53*), the details of which are described in the Supporting Information.

(e) The RC-LH1 complexes containing major Cars ($n = 9-11$, $11 + 13$, and 13) were obtained from *Rba. sphaeroides* G1C, *Rba. sphaeroides* 2.4.1, *Rsp. molischianum*, *Rps. acidophila* 10050, and *Rsp. rubrum* S1, respectively. (i) The RC-LH1 complexes were obtained from *Rba. sphaeroides* G1C, *Rba. sphaeroides* 2.4.1, and *Rsp. molischianum* as follows: The chromatophores of the three strains in 50 mM glycylglycine (pH 7.8; $OD_{850} = 100$ cm^{-1}, 17 mL) were solubilized at 0 °C for 10 min with a mixture of *n*-octyl-β-D-thioglucopyranoside (OTG; Kishida Chemical Co., Ltd., Japan) and sodium cholate (SC; Kishida Chemical Co., Ltd., Japan) whose concentrations were 1.5 and 0.50, 1.5 and 0.50, and 1.0 and 0.33%, respectively. After the addition of 1 equiv volume of the same buffer, each suspension was centrifuged (220000*g*, 4 °C, 1 h). The supernatant was subjected to sucrose density-gradient centrifugation (100000*g*, 4 °C, 19 h) by use of 0.3, 0.6, 0.9, and 1.2 M sucrose layers containing 0.3% OTG and 0.2% SC. In *Rba. sphaeroides* G1C and 2.4.1, two bands originating from the monomer and the dimer appeared, the latter of which was collected. (ii) The RC-LH1 complexes from *Rps. acidophila* 10050 and *Rsp. rubrum* S1 were obtained following the method described previously (*54*). Chromatophores in 20 mM Tris-HCl (pH 8.0; OD_{860} and $OD_{880} = 20$ cm^{-1}, respectively) were solubilized with 1% *N*,*N*-dimethyldodecylamine-*N*-oxide (LDAO; Fluka Chemie GmbH, Germany) at 27−28 °C for 30 min. After centrifugation (23000*g*, 4 °C, 10 min), the supernatant was subjected to sucrose density-gradient centrifugation (206000*g*, 4 °C, 16 h) by the use of 0.4, 0.6, 0.8, and 1.0 M sucrose layers containing 1% SC. The crude RC-LH1 was purified by DE52 ion-exchange column chromatography (Whatman International Ltd., United Kingdom).

Determination of Car Compositions in the Pigment−Protein Complexes. The Cars in pigment−protein complexes were extracted by the method described previously (*54*) with some modifications: The suspension of each pigment−protein complex ($OD = 10$ cm^{-1} at the Q_y absorption) was loaded onto a DE52 column, washed with distilled waster, and purged with N_2 gas to facilitate the complete binding of the pigments to the column. For complete removal of Cars, the column was washed with acetone and then benzene until it became colorless. After it was dried with anhydrous Na_2SO_4, the solution was concentrated by purging N_2 gas and then applied to alumina column chromatography (Alminum oxide 90 standardized; Merck KGaA, Germany) to remove BChl *a* and lipids; Cars were eluted by the use of a diethyl ether/benzene mixture. This column chromatography was repeated twice. The eluent was dried by purging N_2 gas, dissolved into the eluent, and subjected to high-pressure liquid chromatography (HPLC).

The Car extracts were analyzed by an HPLC apparatus equipped with a diode array detector (Waters 996; Waters Corp., United States) under the following conditions: column, a 4.6 mm i.d. × 250 mm column packed with Lichrosorb Si-60 (5 μs; Merck GmbH); eluent, 1% acetone in benzene; the flow rate, 0.5 mL/min; and the detection wavelength, 350−800 nm.

Submicrosecond Time-Resolved Absorption Spectroscopy of T_1 Cars in Solution and in Pigment−Protein Complexes. (a) Time-Resolved Absorption Measurements. The setup for time-resolved absorption measurements was described previously (*55*). A dye laser (Lambda Physik FL-2003; pulse duration, 12 ns; repetition rate, 2 Hz) was pumped by the second harmonic (532 nm) of a Nd:YAG laser (Lumonics HY-400; pulse duration, 12 ns; and repetition rate, 2 Hz). The 781 nm pulses for excitation of BChl *a* in solution to the Q_y state were generated by the use of LDS765 (Nippon Kankoh Shikiso Kenkyusho, Japan), whereas the 850, 881, 868, and 881 nm pulses, for excitation of BChls in the LH2, LH1, RC, and RC-LH1 complexes, respectively, to the Q_y state were generated by the use of LDS867 (Hayashibara Biochemical Laboratories, Inc., Japan); the output power was 1.0−1.2 mJ/pulse. In recording time-resolved spectra, a 200 ns gate was used for Cars in solutions, whereas a 50 ns gate was used for the pigment−protein complexes. A total of 60 time-resolved spectra were recorded for each sample: 10 times data accumulation for Cars in solution and 40 times

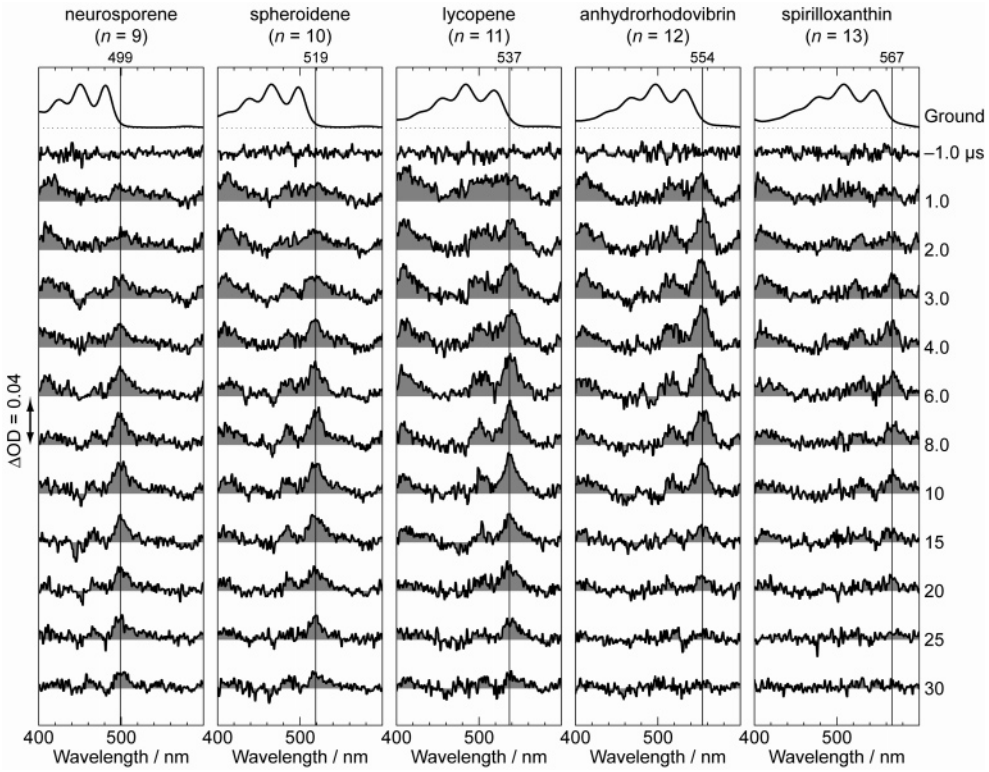

FIGURE 1: Submicrosecond time-resolved absorption spectra of all-*trans* neurosporene ($n = 9$), spheroidene ($n = 10$), lycopene ($n = 11$), anhydrorhodovibrin ($n = 12$), and spirilloxanthin ($n = 13$) in benzene solution (3×10^{-5} M); BChl *a* (3×10^{-5} M) was used as a triplet sensitizer. The sensitizer was excited, in the Ar atmosphere, at the Q_y absorption (781 nm). The ground-state spectra are shown on the top for comparison.

data accumulation for pigment−protein complexes to obtain one time-resolved spectrum. The sample solution was circulated between a flow cell (optical path length, 2 mm) and a reservoir.

(b) Preparation of Deoxygenated Sample Solution and Suspensions. (i) Each Car ($n = 9-13$) and BChl *a* (the sensitizer) were dissolved in benzene (spectral grade; Kishida Chemical Co., Ltd., Japan) at a concentration of 3×10^{-5} M. Before each measurement, benzene-saturated high-purity Ar gas (>99.999%) was bubbled through the sample solution (20 mL) for 40 min; the bubbling continued during the measurement.

(ii) Each pigment−protein complex was resuspended into 0.25% sucrose monocholate (Kishida Chemical Co., Ltd.) in 20 mM Tris-HCl (pH 8.0); the concentrations were OD $= 10$ cm^{-1} at 850, 881, 800, and 881 nm for the LH2, LH1, RC, and RC-LH1 complexes, respectively. In the measurement under the reducing conditions, 400 and 50 mM Na ascorbate was added to the suspensions of the RC and RC-LH1 complexes, respectively. Each sample suspension (10 mL) was degassed by a freeze−thaw technique under the reduced pressure by the use of an aspirator; this procedure was repeated three times to completely remove the atmospheric oxygen. Then, high-purity Ar gas (>99.999%) was bubbled through the suspension for 3 h. Each sample solution or suspension was measured three times to reproducibly obtain the longest T_1 lifetime.

RESULTS

Ground-State and Triplet-State Absorption Spectra of Cars in Solution and in Pigment−Protein Complexes. (a) Cars (n = 9−13) in Solution. Figure 1 shows microsecond time-resolved absorption spectra of typical bacterial Cars, including all-*trans* neurosporene ($n = 9$), spheroidene ($n = 10$), lycopene ($n = 11$), anhydrorhodovibrin ($n = 12$), and spirilloxanthin ($n = 13$) in benzene solution. The ground-state absorption spectra of the set of Cars are shown on the top of the time-resolved spectra for comparison. In order to generate the T_1 state of each Car, the same amount of BChl *a* was added as a sensitizer, and it was then excited at the Q_y absorption (781 nm) in the Ar atmosphere. In the time-resolved spectra, transient absorption due to ^{3}BChl that appears in the shorter wavelength region exhibits a maximum at ~1 μs and then decays, whereas transient absorption due to ^{3}Car appearing in the longer wavelength region rises, reaches a maximum later, and decays. Table 2 lists the wavelengths of the $1B_u^+(0) \leftarrow 1A_g^-(0)$ and $T_n(0) \leftarrow T_1(0)$ absorptions, both shifting to the red with *n*. Table 3 lists the T_1 lifetime (the decay time constant of the $T_n \leftarrow T_1$ absorption), which decreases with *n*. [To avoid an anomaly in the set of T_1 lifetimes of those Cars, the Car concentration in benzene as well as the pump power for BChl excitation were kept to a minimum, which resulted in such a low S/N ratio of the time-resolved spectra.]

(b) Cars (n = 9−11) in Isolated LH2 Complexes. Figure 2 shows submicrosecond time-resolved absorption spectra of the LH2 complexes from *Rba. sphaeroides* G1C, *Rba. sphaeroides* 2.4.1, *Rsp. molischianum*, and *Rps. acidophila* 10050. The spectra were recorded, in the Ar atmosphere, after excitation at the Q_y absorption of BChl (850 nm). Table 1a lists the Car compositions in those LH2 complexes; Cars with $n = 9$, $n = 10$, $n = 11$, and $n = 11$ predominate in those complexes, respectively. The unique spectral pattern of all-*trans* Cars, consisting of the $T_n \leftarrow T_1$ absorption and

Table 2: Conjugation-Length (n) Dependence of (a) $1B_u^+(0) \leftarrow 1A_g^-(0)$ and (b) $T_n(0) \leftarrow T_1(0)$ Absorption (in nm) for Cars in Solution and in Pigment−Protein Complexes

	Cars[a]				
	$n = 9$	$n = 10$[c]	$n = 11$	$n = 12$	$n = 13$[f]
	(a) $1B_u^+(0) \leftarrow 1A_g^-(0)$ absorption				
hexane	468 (neu)	484 (sph)	502 (lyc)	516 (anh)	526 (spx)
benzene	481 (neu)	498 (sph)	518 (lyc)	532 (anh)	545 (spx)
LH2	490 (neu)[b]	510 (sph)	529 (lyc + rhd)[d]		
			523 (lyc + rhd-g)[e]		
LH1	483 (met-neu)	502 (sph)	518 (4H-spx)	531 (anh)	548 (spx)
RC	485 (neu)[b]	503 (sph)			∼534 (spx)
RC-LH1	486 (neu)[b]	505 (sph)	522 (lyc + rhd)		546 (spx)
			521 (lyc + rhd-g)[e]		
	(b) $T_n(0) \leftarrow T_1(0)$ absorption				
acetone	486 (neu)	506 (sph)	523 (lyc)	540 (anh)[g]	559 (spx)[h]
benzene	499 (neu)	519 (sph)	537 (lyc)	554 (anh)	567 (spx)
LH2	511 (neu)[b]	533 (sph)	553 (lyc + rhd)[d]		
			548 (lyc + rhd-g)[e]		
LH1	504 (met-neu)	524 (sph)	545 (4H-spx)	562 (anh)	578 (spx)
RC	523 (neu)[b]	543 (sph)			589 (spx)
core	506 (neu)[b]	527 (sph)	544 (*)[d]		576 (spx)
LH1			543 (*)[e]		576 (spx)[e]
core	524 (neu)[b]	546 (sph)	561 (*)[d]		590 (spx)
RC					598 (spx)[e]

[a] See Table 1 for the abbreviations of Car names. An asterisk indicates a Car with $n = 11$. Abbreviations: met-neu, methoxyneurosporene; and 4H-spx, tetrahydrospirilloxanthin. [b] *Rba. sphaeroides* G1C. [c] *Rba. sphaeroides* 2.4.1. [d] *Rsp. molischianum*. [e] *Rps. acidophila* 10050. [f] *Rsp. rubrum* S1. [g] Ten percent benzene. [h] Fifty percent benzene each was added to increase solubility.

Table 3: Conjugation-Length (n) Dependence of T_1 Lifetimes (in μs) of Cars in Solution and in Pigment−Protein Complexes[a]

	Cars				
	$n = 9$	$n = 10$	$n = 11$	$n = 12$	$n = 13$
benzene	18.5 (neu)	13.5 (sph)	10.0 (lyc)	7.4 (anh)	6.0 (spx)
LH2	9.6 (neu)	6.2 (sph)	4.5 (lyc + rhd)		
			4.2 (lyc + rhd-g)		
LH1	7.6 (met-neu)	5.6 (sph)	4.0 (4H-spx)	3.3 (anh)	2.9 (spx)
RC	6.3 (neu)	4.7 (sph)			2.3 (spx)
core LH1	5.3 (neu)	4.6 (sph)	3.8 (*)		3.1 (spx)
core RC	4.1 (neu)	4.0 (sph)			4.0 (spx)
					4.1 (spx)

[a] See Table 1 for the abbreviations of Car names and Table 2 for the labeling of strains.

the bleaching of the $1B_u^+ \leftarrow 1A_g^-$ absorption, is clearly seen. The transient absorption of each ^{3}Car exhibits a maximum even after 0.2 μs, showing extremely rapid triplet-energy transfer from ^{3}BChl to Car in this complex. The intensity of the spectral pattern is much higher in *Rsp. molischianum* than in *Rps. acidophila*; the difference may reflect the different compositions of Cars that have different binding characteristics (see Table 1a). The wavelengths of the $1B_u^+(0) \leftarrow 1A_g^-(0)$ and $T_n(0) \leftarrow T_1(0)$ absorptions are listed in Table 2, while the T_1 lifetimes are listed in Table 3. Both decrease with n.

(c) Cars ($n = 9-13$) in Reconstituted LH1 Complexes. Figure S1 in the Supporting Information shows the ground-state absorption spectra of the reconstituted LH1 complexes. Into the LH1 complex from *Rps. rubrum* G9 (a Carless mutant), a set of Cars including all-*trans* methoxyneurosporene ($n = 9$), spheroidene ($n = 10$), tetrahydrospirilloxanthin ($n = 11$), anhydrorhodovibrin ($n = 12$), and spirilloxanthin ($n = 13$) were incorporated. All of those Cars have the methoxy group at the end of the conjugated chain to stabilize the binding to the β-peptide. In comparison to the previous reconstitution using neurosporene ($n = 9$) and lycopene ($n = 11$; *50*, *51*), the replacement of those Cars by methoxyneurosporene and tetrahydrospirilloxanthin caused the red-shift of the Q_y absorption (879 → 881 nm and 877 → 882 nm), indicating a much stronger Car-to-BChl intermolecular interaction. The wavelengths of the $1B_u^+(0) \leftarrow 1A_g^-(0)$ absorption for the Cars incorporated into the LH1 complex are listed in Table 2a. The reconstituted LH1 complex is supposed to form a closed ring consisting of 16 subunits as in the case of the LH1 complex isolated from *Rhodobium marinum* (*54*).

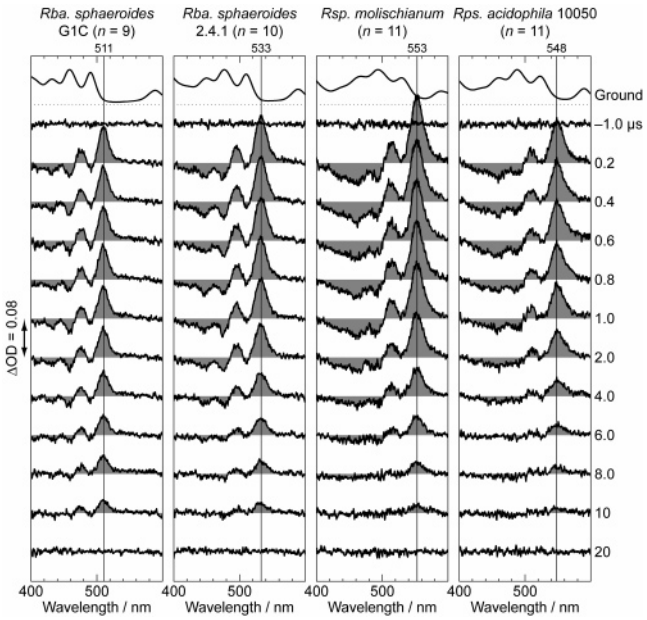

FIGURE 2: Submicrosecond time-resolved absorption spectra of the LH2 complexes from *Rba. sphaeroides* G1C, *Rba. sphaeroides* 2.4.1, *Rsp. molischianum*, and *Rps. acidophila* 10050 containing major Cars, neurosporene ($n = 9$), spheroidene ($n = 10$), rhodopin ($n = 11$), and rhodopin glucoside ($n = 11$), respectively (see Table 1a for the Car composition). The time-resolved spectra were recorded, in the Ar atmosphere, after excitation at the Q_y absorption (850 nm). The ground-state absorption spectra are shown on the top for comparison.

Figure 3 shows the submicrosecond time-resolved absorption spectra of the reconstituted LH1 complexes. The spectra were recorded, in the Ar atmosphere, after excitation at the Q_y absorption of BChl (881 nm). The spectral patterns of ^{3}Cars in those LH1 complexes are similar to those in the LH2 complexes (Figure 2). Both the wavelength of the $T_n \leftarrow T_1$ absorption and the T_1 lifetime in each LH1 complex are shorter than those in each LH2 complex, containing Car with $n = 9$, 10, or 11 (see Tables 2 and 3). In the set of LH1 complexes, the intensity of the $T_n \leftarrow T_1$ absorption tends to become higher in longer chain Cars, probably reflecting higher quantum yields of generating the T_1 state from the singlet $1B_u^-$ state (*51*) and possibly reflecting higher molar extinction coefficients.

(d) Cars ($n = 9$, 10, and 13) in Isolated RCs. Figure S2 in the Supporting Information shows the ground-state absorption spectra of the RCs from *Rba. sphaeroides* G1C, *Rba. sphaeroides* 2.4.1, and *Rsp. rubrum* S1. HPLC analysis showed that neurosporene ($n = 9$), spheroidene ($n = 10$), and spirilloxanthin ($n = 13$) are predominant in those RCs (Table 1b). Figure 4 shows submicrosecond time-resolved

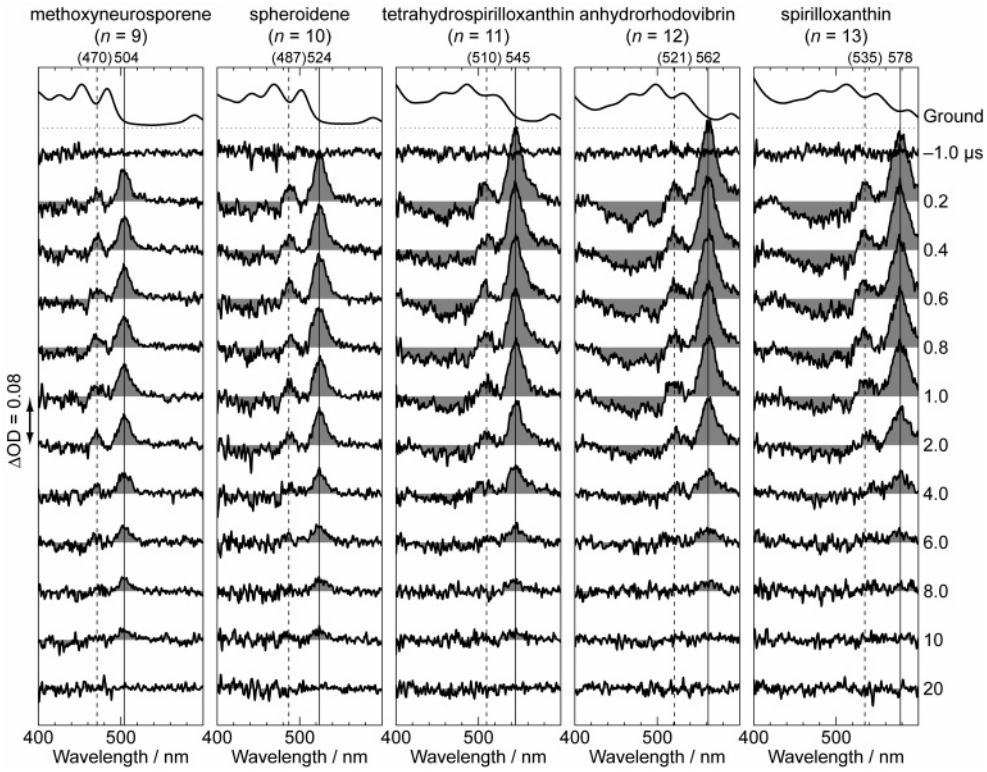

FIGURE 3: Submicrosecond time-resolved absorption spectra of the reconstituted LH1 complexes recorded, in the Ar atmosphere, after excitation at the Q_y absorption (881 nm). The ground-state absorption spectra, on the top for comparison, are reproduced from Figure S1 in the Supporting Information.

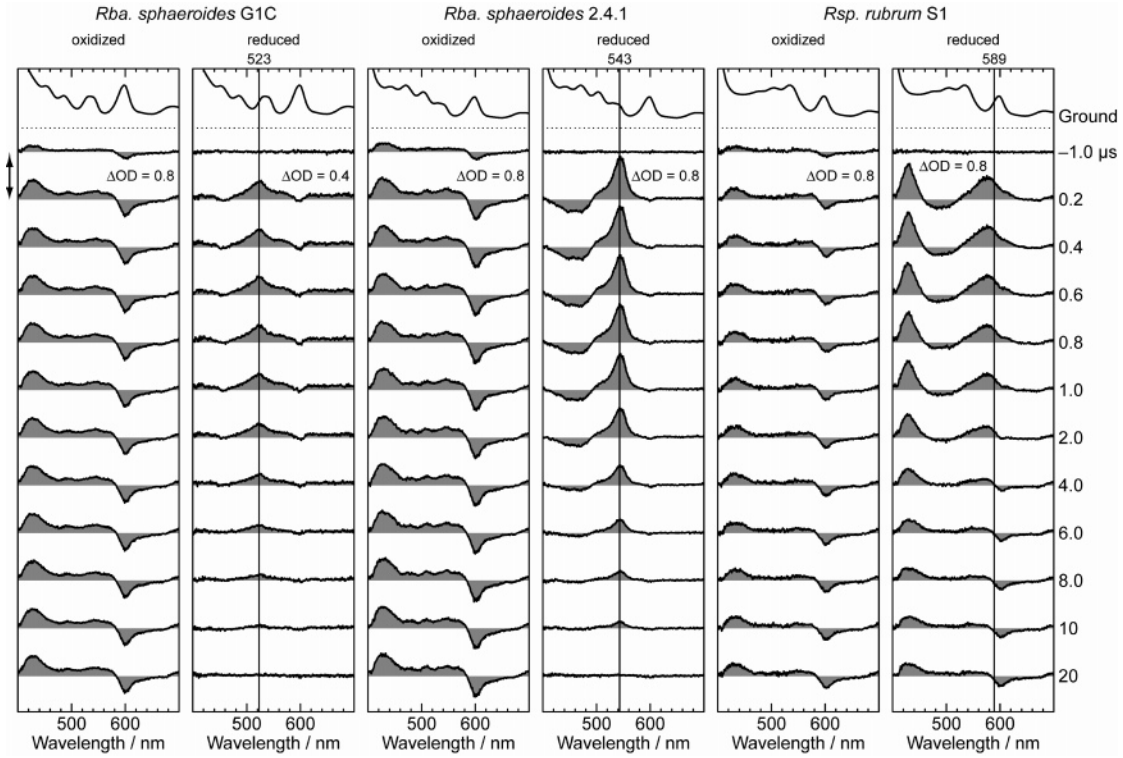

FIGURE 4: Submicrosecond time-resolved absorption spectra of the RCs from *Rba. sphaeroides* G1C, *Rba. sphaeroides* 2.4.1, and *Rsp. rubrum* S1 before and after the addition of 400 mM Na ascorbate (indicated as "oxidized" and "reduced", respectively) recorded, in the Ar atmosphere, after excitation at the Q_y absorption of special-pair BChl (868 nm). The ground-state absorption spectra, on the top for comparison, are reproduced from those in Figure S2 in the Supporting Information.

absorption spectra of each RC before and after the addition of a reducing agent, Na ascorbate (indicated as "oxidized" and "reduced", respectively, in the figure). In the oxidized form (presumably oxidized by atmospheric oxygen), a 428 nm peak is seen even at negative delay time (−1.0 μs, actually 500 ms after excitation, because the sample was excited with 2 Hz repetition); therefore, the peak can be assigned to the special-pair radical cation ($P^{+\bullet}$). In the

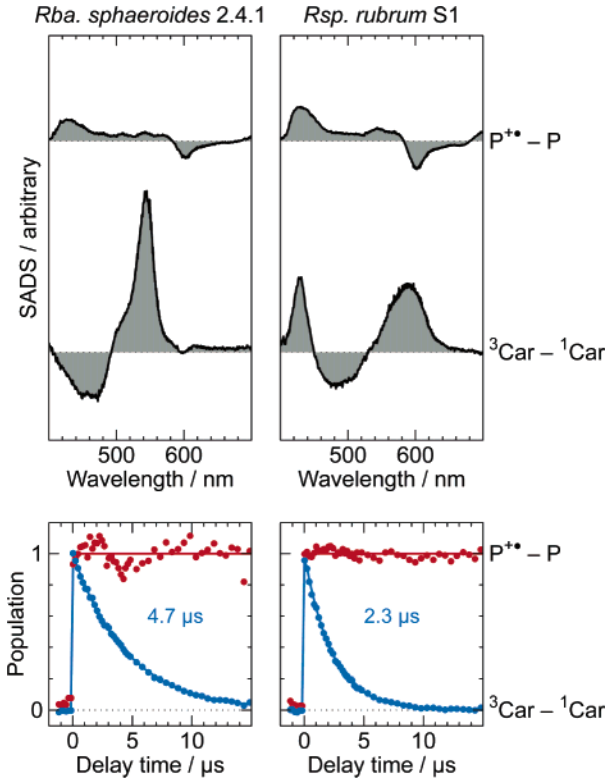

FIGURE 5: SADS and time-dependent changes in population (the initial population is normalized) obtained by the SVD followed by global fitting.

reduced form of RC from *Rsp. rubrum*, a sharp peak appeared at 430 nm immediately after excitation (0.2 μs). In this particular RC, the absorption peak due to $P^{+\bullet}$ and the beaching of the Q_x absorption, both originating from BChl, and the above-mentioned peak and the main $T_n \leftarrow T_1$ absorption, both originating from spirilloxanthin, are overlapped with each other. The precise determination of the T_1 lifetime by the use of time profiles was hampered by this spectral overlap. To determine the spectral patterns and the decay time constants of the two species, we applied singular-value decomposition (SVD) followed by global fitting. Figure 5 (right-hand side) shows the results, i.e., species-associated difference spectra (SADS) and time-dependent changes in population. Because of the extremely long lifetime of $P^{+\bullet}$ as compared to that of ^{3}Car, the two components are practically independent; therefore, the initial population is normalized in the figure. The sharp peak in the SADS can now be definitely assigned to the *cis*-peak of the RC-bound 15-*cis*-spirilloxanthin in the T_1 state; the 580 nm peak can be assigned to the main $T_n \leftarrow T_1$ absorption of this particular isomer. The former and latter peaks can be ascribed to a pair of electronic absorptions, whose transition moments are perpendicular and parallel to the long axis of the molecule, respectively, just like 15-*cis*-β-carotene in the ground state (see Figure 2 of ref *56*). The case of *Rba. sphaeroides* 2.4.1 is also presented for comparison (left-hand side); the *cis*-peak is out of the spectral region recorded. The results indicate that the complete 15-*cis* $\rightarrow$ all-*trans* isomerization in the T_1 state is prevented by the Car binding pocket of the peptides. The T_1 lifetimes of the RC-bound 15-*cis* Cars are systematically shorter than those of the LH-bound all-*trans* Cars (see Table 3).

One of the reviewers suspects that the reducing power of Na ascorbate may not be strong enough to generate the triplet state of the RC-bound Car through charge recombination. It is necessary for the second electron acceptor, Q_A, to be reduced prior to photoexcitation; the midpoint potential of ascorbic acid is approximately +58 mV (*57*), whereas that of Q_A is −50 and −120 ± 20 mV in the RCs from *Rba. sphaeroides* and *Rsp. rubrum*, respectively (*58*). In our experiment, we used an excess amount of Na ascorbate (400 mM), a fact that may have strongly shifted the equilibrium toward the reduction of Q_A. We would like to further investigate this issue by means of time-resolved absorption spectroscopy with a higher time resolution, as has been performed in ref *41*.

(e) Major- and Minor-Component Cars in the RC-LH1 Complexes. As described in the Introduction section, the RC-LH1 complex, whose structure was determined by X-ray crystallography (*6*), is in a monomeric form, and the RC component is surrounded by the C-shaped LH1 component. In our preparation, however, we tried to collect the higher density dimer component, which can be partially decomposed into the lower density monomer component during sample handling. This component may have a S-shaped structure (*59*). In the RC-LH1 complex, the LH1:RC pigment ratio is supposed to be 15:1 in Car and 30:4 = 15:2 in BChl. Therefore, the Car and BChl molecules in the LH1 component must predominate in the electronic absorption spectra of the RC-LH1 complex.

(i) Ground-State Spectra. Figure S3 in the Supporting Information shows the ground-state absorption spectra of the RC-LH1 complexes from *Rba. sphaeroides* G1C, *Rba. sphaeroides* 2.4.1, *Rsp. molischianum*, and *Rps. rubrum* S1 containing the major-component Cars with $n = 9$, $n = 10$, $n = 11$, and $n = 13$, respectively (Table 1c). *Rps. acidophila* contains multiple Cars with $n = 11-13$. The spectral patterns of the LH1 components, having Cars with $n = 9-11$, are definitely different from those of the reconstituted LH1 complexes containing a single kind of Car (Figure S1). In particular, the red-shift of the $1B_u^+ \leftarrow 1A_g^-$ absorption of Cars and the blue-shift of the Q_y absorption of BChls are clearly seen. The results strongly suggest that large changes in the pigment assembly should have taken place on going from the reconstituted LH1 to the LH1 component of the RC-LH1 complex.

(ii) T_1-State Spectra under the Oxidizing Conditions. Figure 6a shows the submicrosecond time-resolved absorption spectra of those RC-LH1 complexes. The spectra were recorded, in the Ar atmosphere, after excitation at the Q_y absorption of BChl (881 nm). No reductant was added to the sample suspensions; therefore, there was no chance for Cars in the RC components to be excited to the T_1 state as in the case of isolated RCs (Figure 4). Therefore, the $T_n \leftarrow T_1$ absorptions in the spectra must specifically originate from Cars in the LH1 components. In the case of the reconstituted LH1 complexes, specific bound Cars with $n = 9-13$ exhibited the $T_n(0) \leftarrow T_1(0)$ absorptions at 504, 524, 545, 562, and 578 nm, respectively (Figure 3). This correlation between the n and the wavelength of the $T_n \leftarrow T_1$ absorption can be used as a guide to assign Car(s) exhibiting the $T_n \leftarrow T_1$ absorption in each LH1 component (Figure 6a). The time-resolved spectra in the figure show that different all-*trans* Cars can be simultaneously excited in some strains. In

reference to Table 1c, Cars can be assigned as follows: (1) The RC-LH1 complex from *Rba. sphaeroides* G1C exhibits the $T_n \leftarrow T_1$ absorptions at 506 and 546 nm, which correspond to ^{3}Cars with $n = 9$ and 11 (in the reconstituted LH1 complexes); the Car composition leads us to the assignment of these Cars to neurosporene and lycopene, respectively. (2) The RC-LH1 complex from *Rba. sphaeroides* 2.4.1 exhibits the $T_n \leftarrow T_1$ absorptions at 527 and 575 nm, corresponding to ^{3}Cars with $n = 10$ and 13; the Car composition leads to the assignment of the Cars to spheroidene and spirilloxanthin, respectively. (3) The RC-LH1 complex from *Rsp. molischianum* shows the $T_n \leftarrow T_1$ absorption at 544 nm, corresponding to ^{3}Cars with $n = 11$; the Car composition leads to the assignment of these Cars to lycopene and/or (hereafter abbreviated by "/") rhodopin. The 509 nm peak can be assigned to the $T_n(1) \leftarrow T_1(0)$ vibrational structure of Cars with $n = 11$ (shown by a vertical broken line). (4) The RC-LH1 complex from *Rps. acidophila* 10050 exhibits a pair of peaks at 543 and 576 nm, corresponding to ^{3}Cars with $n = 11$ and $n = 13$; the Car composition leads to the assignment of these Cars to lycopene/rhodopin glucoside and spirilloxanthin, respectively. (5) The RC-LH1 complex from *Rsp. rubrum* S1 exhibits a peak at 576 nm corresponding to a ^{3}Car with $n = 13$; it can be definitely assigned to spirilloxanthin. The 537 nm peak

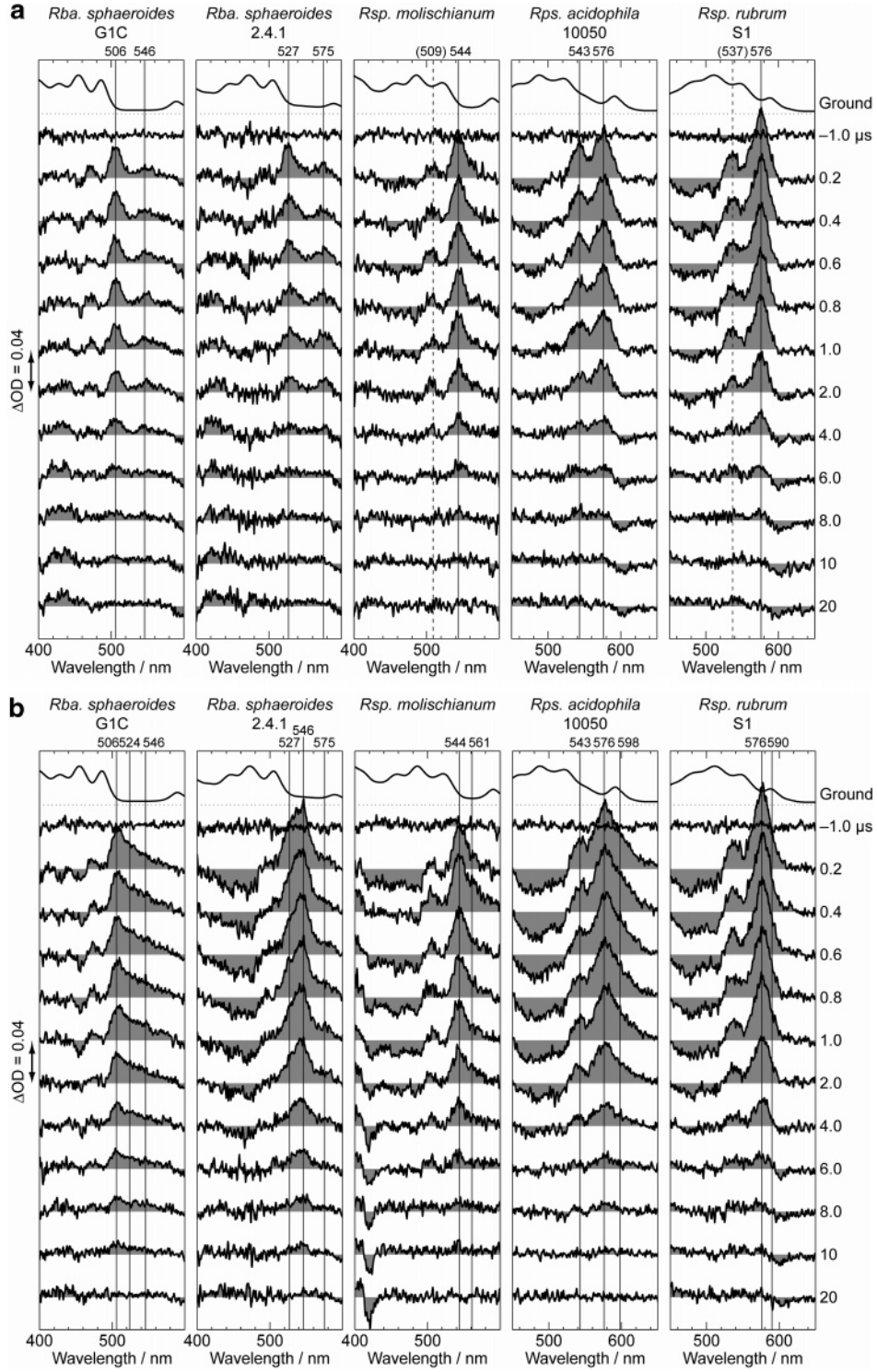

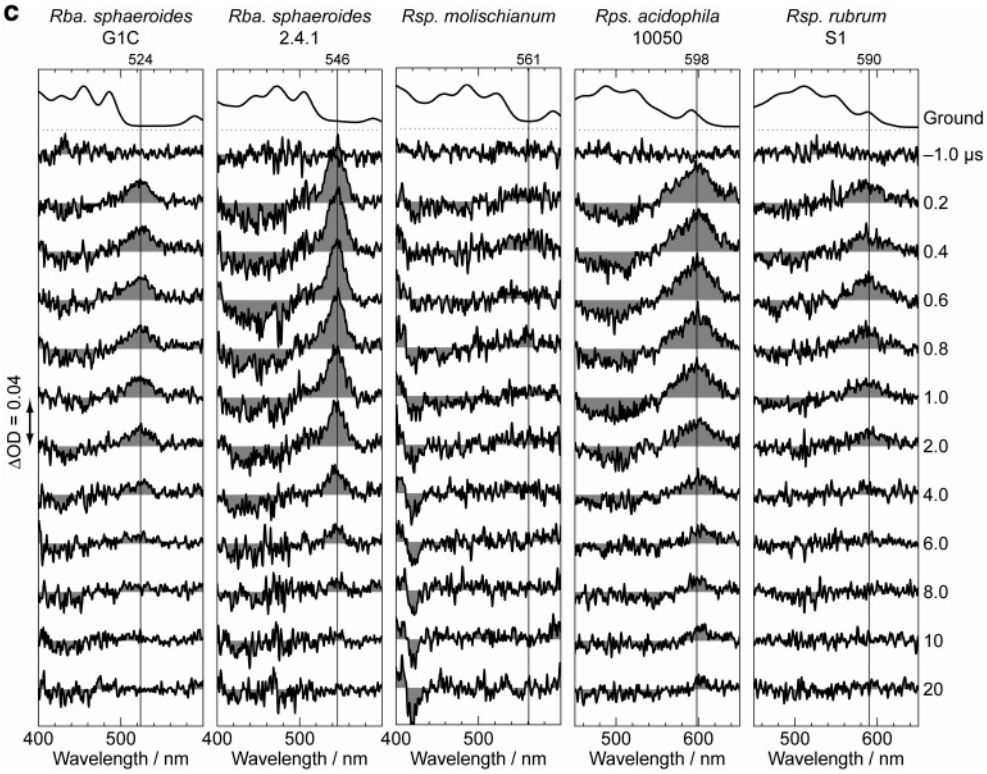

FIGURE 6: Submicrosecond time-resolved absorption spectra of the set of RC-LH1 complexes (a) before and (b) after the addition of 50 mM Na ascorbate and (c) the difference spectra of b − a. The time-resolved spectra, a and b, were recorded, in the Ar atmosphere, after excitation at the Q_y absorption of the LH1 component (881 nm). The ground-state absorption spectra, on the top for comparison, are produced from Figure S3 in the Supporting Information.

can be assigned to the $T_n(1) \leftarrow T_1(0)$ vibrational structure originating from this Car.

Thus, it can be concluded that the $T_n \leftarrow T_1$ absorptions of the major-component ^{3}Car as well as the minor-component ^{3}Car with a much longer ($\Delta n = 2$ or 3) conjugated chain (as a result, with a much lower T_1 energy) can appear in the time-resolved absorption spectra of the LH1 component from *Rba. sphaeroides* G1C and 2.4.1 and in *Rps. acidophila* 10050. When a pair of such Cars is simultaneously populated at the initial stage in *Rba. sphaeroides* G1C or 2.4.1, the Car having a higher energy tends to decay faster than the Car having a lower energy, suggesting triplet-energy transfer from the former to the latter.

Those Cars that are present in the RC-LH1 complexes (Table 1c) but whose $T_n \leftarrow T_1$ absorptions were not identified (Figure 6a) include neurosporene in *Rba. sphaeroides* 2.4.1, anhydrorhodovibrin in *Rps. acidophila*, and anhydrorhodovibrin and rhodovibrin in *Rsp. rubrum*. Each of those minor-component Cars have a T_1 energy higher than that of the major component; therefore, it may not be effectively populated in the T_1 state.

(iii) T_1-State Spectra under the Reducing Conditions. Figure 6b shows the submicrosecond time-resolved absorption spectra of the same set of RC-LH1 complexes, when 50 mM Na ascorbate was added under the same experimental conditions. Figure 6c shows the result of subtraction in each time-resolved spectrum, i.e., "a spectrum recorded with Na ascorbate" minus "a spectrum recorded without Na ascorbate". The remaining peaks after the subtraction can be assigned to the RC-bound 15-*cis* Cars in the T_1 state. Spectral comparison between the $T_n \leftarrow T_1$ absorption of the LH1 component (Figure 6a) and that of the RC component (Figure 6c) leads to a conclusion that the wavelength of the $T_n \leftarrow T_1$ absorption of the RC-bound 15-*cis* Car is longer than that of the LH1-bound all-*trans* Car, when each Car with the same n is considered. In reference to the Car composition (Table 1) and the time-resolved spectra of the isolated RCs (Figure 4), those $T_n \leftarrow T_1$ absorption peaks can be assigned to 15-*cis* neurosporene ($n = 9$), spheroidene ($n = 10$), and an unknown Car ($n = 11$) in the RCs from *Rba. sphaeroides* G1C, *Rba. sphaeroides* 2.4.1, and *Rsp. molischianum*, respectively. The Cars in the RC components of the RC-LH1 complexes from *Rps. acidophila* and *Rsp. rubrum* can be assigned to 15-*cis*-spirilloxanthin ($n = 13$) having the longest conjugated chain.

Conjugation-Length Dependence of the $1B_u^+ \leftarrow 1A_g^-$ and $T_n \leftarrow T_1$ Transition Energies and the T_1 Lifetimes in Solution and in Pigment−Protein Complexes. [Here, in this and the next two subsections, in Tables 2 and 3, and in Figures 7 and 8, we will use the following simplified notations to make comparisons among solutions and pigment−protein complexes more efficient: The isolated LH2 complex → LH2; the reconstituted LH1 complex → LH1; the isolated RC → RC; the LH1 component of RC-LH1 → LH1 in core; and the RC component of RC-LH1 → RC in core.]

(a) Transition Energies. Figure 7 summarizes the $1B_u^+(0) \leftarrow 1A_g^-(0)$ and $T_n(0) \leftarrow T_1(0)$ transition energies (in cm^{-1}), as functions of $1/(2n + 1)$, that have been determined in the present investigation. All of the observed values of wavelengths for the relevant Cars in solution and in pigment−protein complexes, listed in Table 2, are used to draw the energy diagrams. Here, we will focus our attention not on the overall structure but on the conjugation-length (n) of each Car molecule. Because all of the singlet- and triplet-

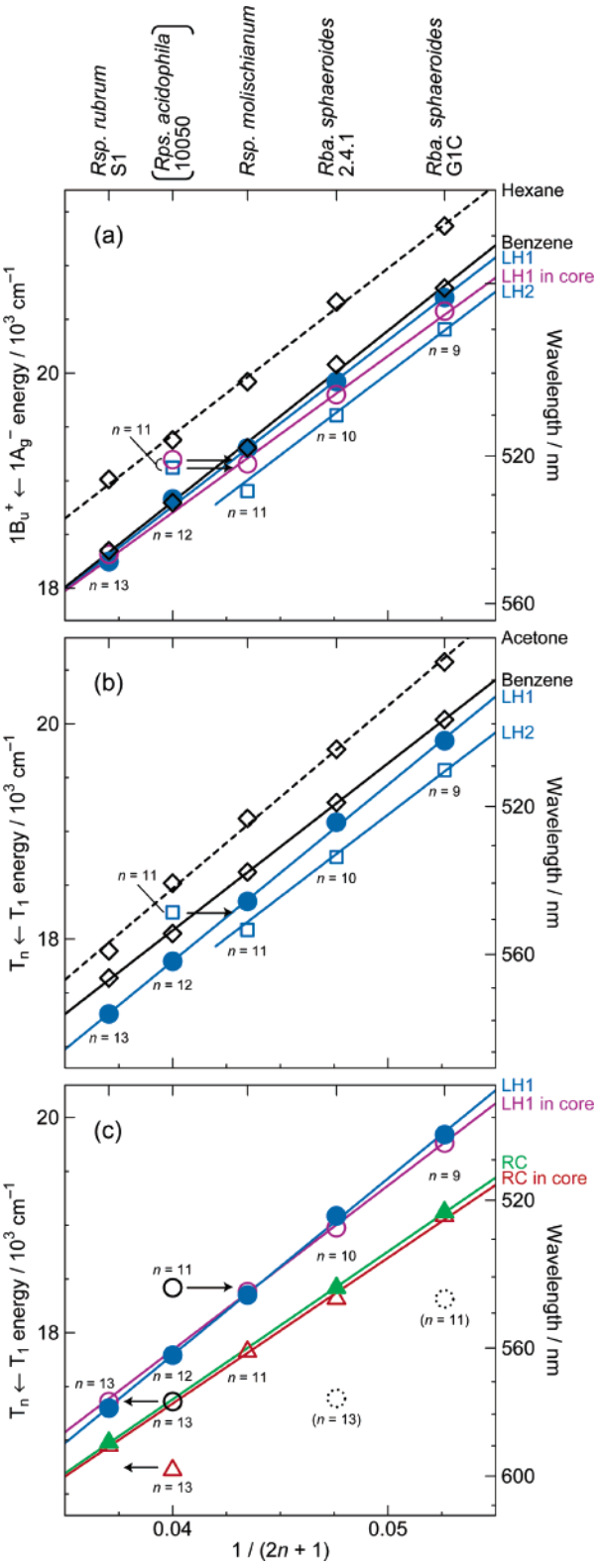

FIGURE 7: (a) $1B_u^+ \leftarrow 1A_g^-$ transition energies of Cars ($n = 9-13$) in *n*-hexane and benzene solutions, Cars ($n = 9-13$) reconstituted into the LH1 complex ("LH1"), Cars ($n = 9-11$) in the isolated LH2 complex ("LH2"), and Cars ($n = 9-11$ and 13) in the LH1 components of the RC-LH1 complexes ("LH1 in core"). (b,c) The $T_n \leftarrow T_1$ transition energies of Cars in acetone and benzene solutions, in LH1, LH2, RC, LH1 in core, and Cars ($n = 9-11$ and 13) in the RC components of the RC-LH1 complexes ("RC in core"). In each conjugation-length dependence, the transition energy is shown as a function of $1/(2n + 1)$. [To the acetone solutions of anhydrorhodovibrin and spirilloxanthin, 10 and 50% benzene was added to increase the solubility.]

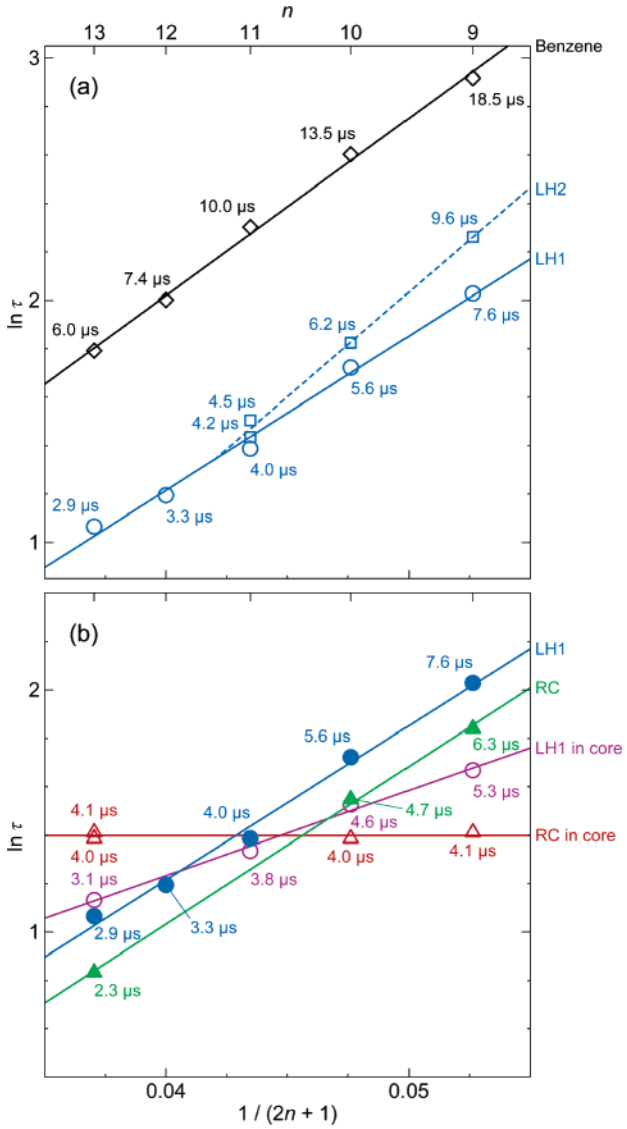

FIGURE 8: Lifetimes (τ) of the $T_n \leftarrow T_1$ absorption of (a) Cars ($n = 9-13$) in benzene solutions and in the reconstituted LH1 complexes ("LH1"), Cars ($n = 9-11$) in the LH2 complexes ("LH2"), Cars ($n = 9$, 10, and 13) in the RC ("RC"), and Cars ($n = 9-11$ and 13) in the LH1 and RC components of the RC-LH1 complexes ("LH1 in core" and "RC in core"). In each conjugation-length dependence, ln τ is shown as a function of $1/(2n + 1)$.

energy levels of Cars (polyenes) can be expressed as linear functions of $1/(2n + 1)$ as described in the Introduction section, the above singlet and triplet transition energies should also exhibit such linear dependence. [Here, we will call the dependence of the transition energies as functions of $1/(2n + 1)$ simply "the linear dependence".] The observed linear dependence of those transition energies can be summarized as follows.

(i) The $1B_u^+ \leftarrow 1A_g^-$ Transition Energies (Figure 7a). (1) A set of all-*trans* Cars with $n = 9-13$ in solutions gives rise to a pair of parallel linear dependence. It shifts to the lower energies on going from *n*-hexane to benzene, reflecting the Car-to-solvent dispersive interaction (*60*, *61*). (2) On going from benzene solution to LH1, the linear dependence slightly shifts to the lower energies. (3) On going from LH1 to LH2, the linear dependence shifts further to the lower energies. (4) In LH1 in core, the slope of the linear relation becomes slightly gentler than in LH1.

(ii) The $T_n \leftarrow T_1$ Transition Energies (Figure 7b,c). (1) The set of bacterial Cars in both acetone/benzene and benzene solutions gives rise to linear relations, the difference between them being ascribable to the effect of dispersive interaction. (2) In LH1, the linear relation shifts to the lower energies in comparison to that in benzene solution. (3) In LH2, the linear relation shifts further to the lower energies parallel to that of benzene solution. (4) In LH1 in core, the linear dependence becomes slightly gentler than in LH1, exhibiting a crossing point at $n = 11$. (5) The linear dependence is almost unchanged on going from RC to RC in core.

(b) T_1 Lifetimes. A linear dependence of ln τ (where τ is the lifetime) as a function of $1/(2n + 1)$ is anticipated for the following reasons: The energy-gap law proposed by Englman and Jortner (*62*) is given by

$$k = \frac{2\pi}{\hbar} C^2 \frac{1}{\sqrt{2\pi\Delta E\hbar\omega}} \exp\left(-\frac{1}{2}\delta^2\right) \exp\left(-\frac{\gamma\Delta E}{\hbar\omega}\right) \quad (1)$$

with

$$\gamma \equiv \ln\frac{2\Delta E}{\delta^2\hbar\omega} - 1 \ (>0)$$

where k is the rate of internal conversion, C is the nonadiabatic vibronic-coupling constant, ΔE is the energy gap between the initial and the final states, ω is the adiabatic angular frequency of the accepting mode, and δ is the displacement of the potential minimum along the normal coordinate upon transition. Equation 1 leads to a linear relation

$$\ln(\tau/\sqrt{\Delta E}) = \frac{\gamma}{\hbar\omega}\Delta E + \text{const} \quad (2)$$

Neglecting change in $-\ln(\sqrt{\Delta E})$, a more simplified linear relation can be obtained as

$$\ln\tau = a \cdot \Delta E + b \quad (3)$$

where a and b are constants. Because ΔE is a linear function of $1/(2n + 1)$ as mentioned above, it can be rewritten as

$$\ln\tau = a'/(2n + 1) + b \quad (4)$$

Thus, the linear dependence is derived. Figure 8 summarizes the T_1 lifetimes that have been determined in the present investigation. The anticipated linear dependence of ln τ is clearly seen as functions of $1/(2n + 1)$ [here, we simply call the linear dependence of ln τ as a function of $1/(2n + 1)$ "the linear dependence"]. The observed linear dependence can be summarized as follows.

(i) Figure 8a. (1) The linear dependence holds in the set of all-*trans* Cars in benzene solution. (2) In LH2, the T_1 lifetimes are shortened substantially, and the slope of the linear dependence becomes slightly steeper in comparison to that in solution. (3) On going from LH2 to LH1, the slope of the linear dependence becomes gentler, keeping the decay time constant at $n = 11$ almost unchanged.

(ii) Figure 8b. (1) The linear dependence of all-*trans* Cars in LH1 shifts to shorter lifetimes in 15-*cis* Cars in RC, keeping the slope of the linear dependence almost unchanged. (2) On going from LH1 to LH1 in core, the slope of the linear dependence becomes substantially gentler, the decay time constants at $n = 11$ and $n = 13$ being almost unchanged. (3) On going from RC to RC in core, the linear dependence becomes canceled out, a surprising observation.

In all of the cases in solution and in the pigment−protein complexes, a set of Cars with n in the region of 9−13 exhibits the linear dependence. The results indicate that the set of Cars is in a very similar environment except for the intrinsic T_1 energy. A small change in the slope of the linear dependence suggests that another conjugation length-dependent factor may become involved. A drastic change in the slope strongly suggests that a new scheme of triplet-energy dissipation must be introduced.

Possible Mechanisms of Triplet-Energy Dissipation: Modeling and Simulation of the Observed Changes in the Linear Dependence of the T_1 Lifetime: (a) In Solution → LH2. On going from benzene solution to LH2, the T_1 lifetimes become substantially shortened (Figure 8a). We tried to explain this in terms of twisting of the conjugated chain in the LH2-bound all-*trans* Car (see the Supporting Information for the details). Briefly, we first showed that the twisting around the double and single bonds can generate spin−orbit coupling (J in cm^{-1}) due to the mixing of the σ and π orbitals, and as a result, it can enhance ISC. The J values were calculated to be 0.15, 0.32, and 0.54 cm^{-1} for the rotational angles of 15, 30, and 45° around a double bond, whereas they were calculated to be 0.12, 0.23, and 0.32 cm^{-1} for the rotational angles of 15, 30, and 45° around a single bond. For multiple double and single bonds, the values became additive (subtractive) for rotations in the same (opposite) direction. By the use of the Englman and Jortner equation (*62*), we could estimate the rate of ISC (k in s^{-1}) by the use of an equation, $k = 6.58 \times 10^6 J^2$.

Then, we evaluated the rate of ISC due to the overall twisting of the conjugated chain in rhodopin glucoside ($n = 11$) bound to the LH2 complex from *Rps. acidophila* 10050 (*4*); the decay time constant was calculated to be $\tau = 1/k = 29.6$ μs. The J value in solution was set zero by assuming a flat conformation, in which the fluctuation of the rotational angles was neglected. This value can shift the observed lifetime of 10.0 μs in solution to an expected value of 7.5 μs in LH2; the shift was still too small. It should be emphasized, however, that the above calculation was based on the rotational angles in the ground state that had been determined by X-ray crystallography (*4*).

Our previous Raman spectroscopy and normal-coordinate analysis of S_0 and T_1 spheroidene in solution and in RC (*17*) identified large changes, upon triplet excitation, in stretching force constants (or in other words, in bond orders), especially in the central part of the conjugated chain (we call it "the triplet-excited region"); in the triplet-excited region, the double bonds become more single bondlike and the single bonds become more double bondlike (see Figure 7a in ref *17*). Therefore, triplet excitation can cause much stronger twisting of the conjugated chain due to the elongation of central double bonds reducing the barrier to rotation. A 1.9 times increase in the J value due to a stronger twisting of the conjugated chain may suffice to shorten the lifetime from the value in solution (10.0 μs) to the observed value in LH2 (4.2 μs) shown in Figure 8a.

(b) LH2 → LH1. On going from LH2 to LH1, the T_1 lifetime in Car with $n = 9$ is substantially shortened, keeping

almost the same lifetime in Car with $n = 11$ (Figure 8a). Each LH2 contains one kind of Car having a particular n as the major component (see Table 1a), and each LH1 was specifically reconstituted with one kind of Car. Therefore, the above change needs to be explained in terms of a single kind of Car with $n = 9$, for example, in either LH1 or LH2.

There are a couple of factors to be considered to explain this observation. (i) The $1B_u^+ \leftarrow 1A_g^-$ absorption is blue-shifted in LH1 rather than in LH2 (Figure 8a), suggesting that the dispersive interaction is weakened in LH1. (ii) As mentioned in the preceding subsection, changes in bond orders take place upon triplet excitation. Actually, the changes in bond orders are much larger in Car with $n = 9$ than in Car with $n = 11$, especially in the triplet-excited region (see Figure 6 of ref *63*). (iii) The quantum yields of triplet generation for Cars with $n = 9$, $n = 10$, and $n = 11$, which were 10, 12, and 17% in LH2 increased up to 19, 20, and 27% in LH1 (see Table 1 of ref *51*). Therefore, on going from LH2 to LH1, the $T_1 \rightarrow S_0$ ISC should be accelerated, and more importantly, the shortest chain Car with $n = 9$ generates the least amount of triplet.

Thus, more efficient ISC in LH1 than in LH2 can be explained in terms of the weakening of the dispersive interaction and the lengthening of double bonds upon triplet excitation, both facilitating the twisting of the conjugated chain. The observed decrease in the T_1 lifetime of Car with $n = 9$, which is larger than that of Car with $n = 11$, can be explained in terms of further lengthening of the central double bonds upon triplet excitation as well as a smaller amount of triplet energy to be dissipated.

(c) LH1 → RC. The linear dependence in all-*trans* Cars in LH1 shifts to the shorter lifetimes in 15-*cis* Cars in RC, keeping the slope almost unchanged (Figure 8b). As mentioned in the Introduction section, the detailed mechanism of triplet-energy dissipation in the RC-bound 15-*cis*-spheroidene ($n = 10$), which includes the rotational motions around the central double bonds, has been proposed (*18*). The parallel shift of the linear relation from all-*trans* Cars in LH1 to 15-*cis* Cars in RC, observed in the present investigation, strongly suggests that the same mechanism is in operation in both 15-*cis*-neurosporene ($n = 9$) and 15-*cis*-spirilloxanthin ($n = 13$), which were identified in the RCs from *Rba. sphaeroides* G1C (*64*) and *Rsp. rubrum* S1 (*65*), respectively.

(d) LH1 → LH1 in Core. On going from LH1 to LH1 in core, the slope in the linear dependence in LH1 becomes much gentler, keeping the values at $n = 11$ and $n = 13$ almost unchanged (Figure 8b). LH1 can incorporate a single Car, neurosporene ($n = 9$), for example, whereas LH1 in core from *Rba. sphaeroides* G1C actually contains both neurosporene ($n = 9$) and lycopene ($n = 11$) as the major- and minor-component Cars. We have succeeded in simulating the substantial shortening of the apparent lifetime in the former Car, assuming a triplet-energy transfer from the former Car to the latter Car (see Scheme 1A).

Briefly, on the basis of the T_1 lifetimes of the set of Cars in LH1, we assumed the intrinsic lifetimes of Cars with $n = 9$ and $n = 11$ to be 7.6 and 4.0 μs, respectively. Then, we could determine, by simulation, the time constant of triplet-energy transfer to be 8.5 μs; here, we applied a constraint that the T_1 state of Car with $n = 11$ needs to be depopulated before the triplet-energy transfer takes place. Then, our simulation showed that the apparent lifetimes of the major-component and minor-component Cars turned out to be 5.30 and 5.35 μs, respectively, in excellent agreement with the observed lifetime in LH1 in core, i.e., 5.3 μs (Figure 8b). The slightly faster decay of the major-component Car than the minor-component Car, observed in Figure 6a (*Rba. sphaeroides* G1C), is also nicely simulated. (See the Supporting Information for the details of simulation.)

Scheme 1

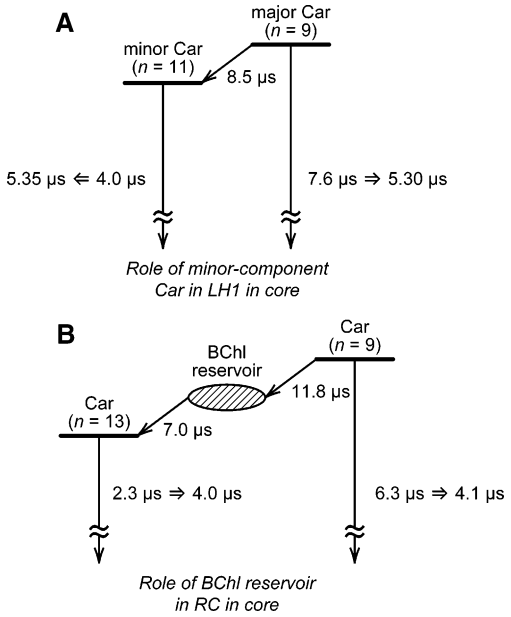

(e) RC → RC in Core. On going from RC to RC in core, a drastic change in the slope of the linear dependence to zero takes place (Figure 8b). To explain this change, a speed-up of the T_1 decay in the shortest chain Car ($n = 9$) and a slow-down of the T_1 decay in the longest chain Car ($n = 13$), for example, need to be demonstrated. Here, we assumed a triplet-energy reservoir, consisting of BChl molecules in the RC, whose T_1 energy is similar to that of ^{3}Car with $n = 11$. Then, we could explain the shortening of the T_1 lifetime in Car with $n = 9$ (having a higher T_1 energy) in terms of a triplet-energy transfer to the reservoir, while the lengthening of the T_1 lifetime in Car with $n = 13$ (having a lower T_1 energy) assuming a triplet-energy transfer from the reservoir (see Scheme 1B). In Car with $n = 9$, the intrinsic lifetime of 6.3 μs could be shortened to an apparent lifetime of 4.1 μs by assuming triplet-energy transfer to the reservoir with a time constant of 11.8 μs. On the other hand, in Car with $n = 13$, the intrinsic lifetime of 2.3 μs could be lengthened to an apparent lifetime of 4.0 μs, assuming triplet-energy transfer from the reservoir with a time constant of 7.0 μs. (A spatial, energetic, and timely justification of assuming such a triplet-energy reservoir will be described in the Discussion section. The details of simulation are described in the Supporting Information.)

DISCUSSION

Development of the Photoprotective Function of Cars in the Bacterial Photosynthetic System. Here, we try to discuss the development of the photosynthetic system consisting of the LH2, LH1, and RC complexes in purple bacteria. (In this section, we abolish the abbreviation used in the previous

subsections.) Concerning the roles of Cars in photosynthesis, we tended, in the past, to emphasize the light-harvesting function of all-*trans* Cars in the LH complexes and the photoprotective function of 15-*cis* Car in the RC (see the Introduction section). Now, we will focus our attention rather on the photoprotective function of all-*trans* Cars in the LH complexes.

(a) LH2 Complex. The LH2 complex, which must have been introduced to the photosynthetic system to collect additional light energy, seems to have developed a way to dissipate the excess triplet energy as well. The singlet internal-conversion processes of all-*trans* Cars in this complex take place in the $10^{-14}-10^{-11}$ s time range; therefore, the Car-to-BChl singlet-energy transfer in the complex needs to be completed within this period of time (*14*, *15*). The rapid internal-conversion processes in the order, either $1B_u^+ \rightarrow 1B_u^- \rightarrow 2A_g^- \rightarrow$ ground $1A_g^-$ (in Cars with $n = 9$ and 10) or $1B_u^+ \rightarrow 3A_g^- \rightarrow 1B_u^- \rightarrow 2A_g^- \rightarrow 1A_g^-$ (in Cars with $n = 11-13$), facilitate a photoprotective function, by themselves, in the sense that Cars do not store the excess singlet energy any longer. In addition, Cars have a channel of singlet-to-triplet conversion (singlet fission or ISC) from the $1B_u^-$ state (*33*, *35*, *66*), and on the other hand, BChl has a high quantum yield of ISC. Both of the resultant ^{3}Car and ^{3}BChl can quench efficiently the Q_y singlet excitation of BChl that is remaining even after singlet-energy transfer, through the singlet−triplet annihilation reaction, another mechanism of photoprotection. Because the T_1 energies of Cars are lower than that of BChl (*19*), the excess triplet energy is eventually collected by Car and dissipated as heat to the surroundings. Figure 8b summarizes the result of our first systematic determination of the T_1 lifetimes of all-*trans* Cars in the LH2 complexes, evidencing triplet-energy dissipation in the 4−10 μs time scale (see Figure 2 for the raw time-resolved spectra).

(b) LH1 Complex. It has been shown that singlet-energy transfer was more efficient in the LH2 complex, whereas the generation of ^{3}Car was more efficient in the LH1 complex (see Table 1 of ref *51*). The former result supports the idea that the LH2 complex is more specialized in the light-harvesting function that is facilitated by holding tightly the all-*trans* Car molecule through stronger dispersive interaction (Figure 7a,b). The latter result is consistent to the present observation that a more efficient method of triplet-energy dissipation is developed in the LH1 complex, the detailed mechanism of which has been described in the previous section. Most probably, the LH1 complex is more specialized in the photoprotective function rather than the light-harvesting function.

(c) RC. Because ^{3}P, sensitizing the generation of $^1O_2$, can be readily formed by reverse electron transfer followed by charge recombination, the quenching of it and dissipating the transferred triplet energy by Car must be most crucial in the RC. Here, the usage of a Car having a 15-*cis*, longer conjugated chain must be absolutely necessary for the most efficient triplet-energy dissipation as described in the Introduction section. A detailed analysis of the triplet-state dynamics of 15-*cis*-spheroidene bound to the RC from *Rba. sphaeroides* 2.4.1 leads us to the finding of a leak channel for triplet-energy dissipation with a time constant as short as 1 μs (*18*).

(d) RC-LH1 Complex. This most basic photosynthetic unit, consisting of the LH1 and RC components, has realized a unique linear dependence of the T_1 lifetime. In the Cars bound to the LH1 component, the linear dependence is suppressed to a minimum, whereas in the Cars bound to the RC component, the linear dependence is completely canceled (Figure 8b). We do not know, at the present stage, how the pressure of natural selection has built such a unique pair of mechanisms that are described in the previous subsection. We would like to propose the following speculative interpretation from the viewpoint of diversity and uniformity.

During the process of evolution, purple photosynthetic bacteria must have started to use Cars having different conjugation lengths (n) to harvest additional light energy in different wavelength regions from a white continuum of sunlight. In other words, habitat segregation may have started to share the light energy, because collecting light energy is a crucial issue for "photosynthetic bacteria". The purple bacteria might have started to use those Cars for the photoprotective function as well, i.e., quenching ^{3}BChl sensitizing the generation of harmful $^1O_2$. Unfortunately, those Cars that are advantageous (disadvantageous) for the light-harvesting function are disadvantageous (advantageous) for the photoprotective function. This is a matter of diversity in the excited-state properties of Cars, which had to be tuned by intermolecular interactions with BChls and peptides.

On the other hand, those photosynthetic bacteria probably had to use basically the same set of machinery, i.e., the RC-LH1 complex, whose basic assembly of the Car, BChl, and peptide molecules must have been very similar immediately after differentiation. As a result, the efficiency of singlet-energy transfer from the LH1 to the RC complex by the use of BChls as well as the efficiency of electron-transfer reaction along the redox components in the RC might have been almost the same. This is a matter of uniformity in the rest of chemical components in the photosynthetic unit.

To achieve a balance, as mush as possible, between the dissipation of the excess triplet energy and the difference in the incoming light energy minus the singlet energy to be used for electron transfer, the best solution might have turned out to make the rate of triplet-energy dissipation in the LH1 and RC component as similar as possible among the set of Cars with $n = 9-13$ being used. This choice should originate from the diversity of Cars as well as the uniformity of the rest of the chemical components.

Comparison to the Results of Previous Investigations. (a) T_1 Lifetimes of the RC-Bound 15-cis-Spheroidene and the LH-Bound All-trans-Spheroidene. Cogdell et al. (*21*) determined the T_1 lifetime of 15-*cis*-spheroidene in the RC to be 4−5 μs, whereas Monger et al. (*31*) determined the T_1 lifetime of all-*trans*-spheroidene in chromatophores to be 7 μs. The former value is in excellent agreement with 4.7 μs determined in the present investigation, and the latter value is in good agreement with 6.2 μs presently determined (Figure 8a,b). Those T_1 lifetimes correspond to the decay time constant through "a slow process of ISC in a fixed conformation" that we defined previously (*17*). Concerning this mechanism, it is worth mentioning that our calculation of the ISC rate due to the twisting of the conjugated chain in the RC-bound 15-*cis*-spheroidene predicted a value of 4.5 μs, in excellent agreement with the observed value. On the other hand, we also defined "a fast process of ISC through

rotational motion" in the 15-*cis* isomer. The difference between the two pathways is most pronounced in solution: The T_1 lifetime of 15-*cis*-spheroidene isomerizing toward all-*trans* is 0.83 μs, whereas that of stable all-*trans*-spheroidene is 4.76 μs (*55*). Actually, we identified the fast process as a leak channel of triplet energy with a time constant of 1 μs in a RC (see ref *18*). Most probably, this process through rotational motion is suppressed in the Car binding pocket, but it still plays a most important role in the dissipation of triplet energy.

(b) Triplet-Energy Transfer among Cars in the LH Complex. Zhang and co-workers (*40*) found, for the first time, triplet-energy transfer from Car ($n = 11$) to Car ($n = 12$) in the LH2 complex from *Rps. palustris*. They used a sequential model, i.e., ^{3}Car ($n = 11$) $\rightarrow$ ^{3}Car ($n = 12$) $\rightarrow$ ^{1}Car ($n = 12$), and determined, by global analysis, the decay time constants of the first and second components to be 0.52 and 1.73 μs under the aerobic conditions, whereas they were 0.76 and 2.10 μs under anaerobic conditions. We also observed triplet-energy transfer from Car ($n = 9$) to Car ($n = 11$) in the LH1 component of the RC-LH1 complex from *Rba. sphaeroides* G1C, for example. In the simulation described in the Results section, we assumed, in addition to the parallel decay from Car ($n = 9$) and Car ($n = 11$) with the intrinsic lifetimes of 7.6 and 4.0 μs, respectively, triplet-energy transfer from the former to the latter (8.5 μs).

They observed a rapid (0.5−0.8 μs) triplet-energy transfer between Cars with $n = 11$ and $n = 12$, whereas we observed a slow (8.5 μs) triplet-energy transfer between Cars with $n = 9$ and $n = 11$. The difference in the triplet energy-transfer time constants and the above modelings originates from the gap in triplet energy between the donor and the accepter due to the difference in the conjugation length, $\Delta n = 1$ in the former and $\Delta n = 2$ in the latter. Because the Car-to-Car edge-to-edge distance is as long as 10.5 Å, the Car-to-Car triplet-energy transfer should be explained only in terms of a superexchange mechanism that is mediated by the intervening BChls.

(c) Triplet-Energy Reservoir Canceling the Conjugation-Length Dependence in the RC Component of the RC-LH1 Complex: Justification. We have explained the speed-up of the triplet-energy dissipation in Car with $n = 9$ and the slow-down of the triplet-energy dissipation in Car with $n = 13$ both in the RC component, assuming a triplet-energy reservoir consisting of BChls. Here, we try to justify this assumption. (i) We focused our attention on the assembly of the special-pair and accessory BChl molecules in close proximity to the 15-*cis*-spheroidene; one of the accessory BChl molecules is actually in contact with the central part of the RC-bound 15-*cis* Car to facilitate triplet-energy transfer (*3*). Therefore, this model of the triplet-energy reservoir is justified spatially. (ii) The T_1 energies of all-*trans* neurosporene ($n = 9$), spheroidene ($n = 10$), and lycopene + rhodopin (both $n = 11$) in the LH2 complexes from *Rba. sphaeroides* G1C, *Rba. sphaeroides* 2.4.1, and *Rsp. molischianum* have been determined to be 7030, 6920, and 6870 cm^{-1}, respectively (*19*). Unfortunately, the T_1 energies of the RC-bound 15-*cis* Cars are still unknown. However, because the $1B_u^+$ energy of the 15-*cis* isomer is slightly higher than that of the all-*trans* isomer, i.e., by 138 cm^{-1} in neurosporene, by 88 cm^{-1} in β-carotene, and by 73 cm^{-1} in spirilloxanthin (see Table 1 in ref *65*), the difference in the T_1 energies between the 15-*cis* and all-*trans* isomers may be very small. On the other hand, the T_1 energies of BChls in the RC have been determined to be 7590 cm^{-1} in *Rba. sphaeroides* R26 and 6680 cm^{-1} in *Rps. viridis* (*67*). Then, it is suggested that the T_1 energy of a Car with $n = 11$, i.e., 6870 cm^{-1}, should be within the tuning range of the T_1 energies of BChls, i.e., 6680−7590 cm^{-1}. The T_1 energy of these BChls may be tuned by the peptide−peptide interaction between the RC component and the LH1 component ("the intercomplex interaction" mentioned in the Introduction section). Thus, the model of triplet-energy reservoir is justified energetically, as well. (iii) The T_1 lifetime of BChl in the RC from *Rba. sphaeroides* is in the region of 148−152 μs, whereas that in the RC from *Rps. viridis* is in the 91−95 μs region (*68*). These lifetimes are long enough for the BChl triplet-energy reservoir to timely function as a buffer.

Finally, it is interesting to note that the $T_n \leftarrow T_1$ absorption is extremely weak in the RC component from *Rsp. molischianum* containing lycopene and rhodopin (both $n = 11$) as shown in Figure 6c. The result supports the idea that the T_1 energy of those Cars is similar to that of the BChl reservoir and that the triplet population of Cars is delocalized over the BChl molecules.

(d) Triplet Generation in the RC-LH1 Complex Controlled by the Redox Environment of the RC. Alric (*41*) succeeded in separately probing the T_1 state of the RC-bound spirilloxanthin and that of the LH2-bound spheroidene (and OH-spheroidene, which is abbreviated in the discussion here for simplicity) by the use of *Rvi. gelatinosus*. In dithionite-reduced membranes, this author could time-resolve, by electronic-absorption spectroscopy, the processes of charge separation ($P^{+\bullet}$ bacteriopheophytin$^{-\bullet}$) followed by charge recombination at P, as well as the triplet generation of the RC-bound spirilloxanthin followed by the LH2-bound spheroidene. At lower (higher) light intensity, T_1 spirilloxanthin (T_1 spheroidene) was preferentially generated. In ferricyanide-oxidized membrane, on the other hand, he observed only the triplet generation in the LH2-bound spheroidene.

His observation parallels to ours in the RC-LH1 complexes: The T_1 state of the LH1-bound all-*trans* Cars was observed under the oxidizing condition, whereas the T_1 state of the RC-bound 15-*cis* Cars was observed under the reducing condition. These observations are in complete agreement with the very initial observation on ^{3}Cars bound to the RC by Cogdell et al. (*21*) as well as that on ^{3}Cars bound to the chromatophore membranes by Monger et al. (*31*). The above results have shown that the LH and RC complexes should generate ^{3}Car based on completely different mechanisms. It is very likely that the generation of ^{3}Car is regulated by the redox potential in the environment of the RC, which can control the incoming singlet energy and the outgoing triplet energy by switching the open and closed forms of the RC.

CONCLUSION

The following answers to the questions addressed in the Introduction section have been obtained.

Question 1: How can the intermolecular interaction in the LH complexes affect the triplet-energy dissipation? The twisting of the conjugated chain that is enhanced by the

elongation of the central double bonds upon triplet excitation, under the influence of the dispersive intermolecular interaction, has been shown to enhance the $T_1 \rightarrow S_0$ ISC and the dissipation of triplet energy. It is suggested that the intermolecular interaction is stronger (weaker) and the twisting is smaller (larger) in the LH2 (LH1) complex, which is more specialized in the light-harvesting (photoprotective) function.

Question 2: What is the function of the minor-component Cars in the LH1 component of the RC-LH1 complex? In the case of *Rba. sphaeroides* G1C having the major-component Car with $n = 9$ and a minor-component Car with $n = 11$, for example, the minor-component Car accelerates the decay of the major-component Car, forming a leak channel.

Question 3: How can the intercomplex interaction, i.e., between the RC and the LH1 components in the RC-LH1 complex, affect the dissipation of the triplet energy by the RC? In the RC component, a reservoir consisting of BChls, whose T_1 energy is tuned to around the T_1 energy of Car ($n = 11$), accelerates the triplet-energy dissipation by the shortest chain Car and suppresses the triplet-energy dissipation by the longest chain Car. As a result, the dependence on n of triplet-energy dissipation is canceled.

In order to establish the proposed mechanisms, concerning "the role of the minor-component Car in the LH1 component" and "the role of the BChl triplet reservoir in the RC component", both in the RC-LH1 complex, a more sophisticated technique of Car reconstitution into this particular complex needs to be developed, in addition to those of the Car reconstitution into the RC and LH1 complexes now available. Then, we can systematically change the pair of conjugation lengths and the composition of Cars in the LH1 component and the conjugation lengths of Cars in the RC component. The results will provide us with deeper insight into the mechanisms.

ACKNOWLEDGMENT

We thank Prof. Richard J. Cogdell for stimulating discussion and Dr. Peng Wang for reading the manuscript. We also thank Hiroyuki Ueda, Takashi Handa, and Yusuke Miyake, undergraduate students of K.G.U., for their contribution in the early stages of this investigation.

SUPPORTING INFORMATION AVAILABLE

The details of (i) sample preparations; (ii) ground-state electronic absorption spectra of the LH1, RC, and RC-LH1 complexes (with Figures S1−S3); (iii) enhanced ISC due to the twisting of the conjugated chain in the LH2-bound all-*trans*-rhodopin glucoside and the RC-bound 15-*cis*-spheroidene; and (iv) suppression of the linear dependence in the correlation in the LH1 and RC components of the RC-LH1 complex (Figure S4). This material is available free of charge via the Internet at http://pubs.acs.org.

REFERENCES

1. Green, B. R., Anderson, J. M., and Parson, W. W. (2003) Photosynthetic membranes and their light-harvesting antennas, in *Light-Harvesting Antennas in Photosynthesis* (Green, B. R., and Parson, W. W., Eds.) pp 1−28, Kluwer Academic Publishers, Dordrecht, The Netherlands.
2. Deisenhofer, J., Epp, O., Miki, K., Huber, R., and Michel, H. (1985) Structure of the protein subunits in the photosynthetic reaction centre of *Rhodopseudomonas viridis* at 3 Å resolution, *Nature 318*, 618−624.
3. Allen, J. P., Feher, G., Yeates, T. O., Komiya, H., and Rees, D. C. (1987) Structure of the reaction center from Rhodobacter sphaeroides R-26: The cofactors, *Proc. Natl. Acad. Sci. U.S.A. 84*, 5730−5734.
4. McDermott, G., Prince, S. M., Freer, A. A., Hawthornthwaite-Lawless, A. M., Papiz, M. Z., Cogdell, R. J., and Isaacs, N. W. (1995) Crystal structure of an integral membrane light-harvesting complex from photosynthetic bacteria, *Nature 374*, 517−521.
5. Koepke, J., Hu, X., Muenke, C., Schulten, K., and Michel, H. (1996) The crystal structure of the light-harvesting complex II (B800−850) from *Rhodospirillum molischianum*, *Structure 15*, 581−597.
6. Roszak, A. W., Howard, T. D., Southall, J., Gardiner, A. T., Law, C. J., Isaacs, N. W., and Cogdell, R. J. (2003) Crystal structure of the RC-LH1 core complex from *Rhodopseudomonas palustris*, *Science 302*, 1969−1972.
7. Frank, H. A., and Cogdell, R. J. (1993) The photochemistry and function of carotenoids in photosynthesis, in *Carotenoids in Photosynthesis*, 1st ed. (Young, A., and Britton, G., Eds.) pp 252−326, Chapman and Hall, London, United Kingdom.
8. Koyama, Y., Kakitani, Y., and Watanabe, Y. Photophysical properties and light-harvesting and photo-protective functions of carotenoids in bacterial photosynthesis: Structural selections, in *Primary Processes of Photosynthesis: Basic Principles and Apparatus* (Renger, G., Ed.) in press.
9. Koyama, Y. (1991) Structures and functions of carotenoids in photosynthetic systems, *J. Photochem. Photobiol. B: Biol. 9*, 265−280.
10. Koyama, Y., and Fujii, R. (1999) *Cis-trans* carotenoids in photosynthesis: Configurations, excited-state properties and physiological functions, in *The Photochemistry of Carotenoids* (Frank, H. A., Young, A. J., Britton, G., and Cogdell, R. J., Eds.) pp 161−188, Kluwer Academic Publishers, Dordrecht, The Netherlands.
11. Furuichi, K., Sashima, T., and Koyama, Y. (2002) The first detection of the $3A_g^-$ state in carotenoids using resonance-Raman excitation profiles, *Chem. Phys. Lett. 356*, 547−555.
12. Tavan, P., and Schulten, K. (1986) The low-lying electronic excitations in long polyenes: A PPP-MRD-Cl study, *J. Chem. Phys. 85*, 6602−6609.
13. Tavan, P., and Schulten, K. (1987) Electronic excitations in finite and infinite polyenes, *Phys. Rev. B 36*, 4337−4358.
14. Koyama, Y., Rondonuwu, F. S., Fujii, R., and Watanabe, Y. (2004) Light-harvesting function of carotenoids in photo-synthesis: The roles of the newly found $1^1B_u^-$ state, *Biopolymers 74*, 2−18.
15. Koyama, Y., and Kakitani, Y. (2006) Mechanisms of carotenoid-to-bacteriochlorophyll energy transfer in the light harvesting antenna complexes 1 and 2: Dependence on the conjugation length of carotenoids, in *Chlorophylls and Bacteriochlorophylls: Biochemistry, Biophysics, Functions and Applications* (Grimm, B., Porra, R. J., Rüdiger, W., and Scheer, H., Eds.) pp 431−443, Springer, Dordrecht, The Netherlands.
16. Koyama, Y., Kakitani, Y., and Nagae, H. (2006) Mechanisms of *cis-trans* isomerization around the carbon-carbon double bonds via the triplet state, in *cis-trans Isomerization in Biochemistry* (Dugave, C., Ed.) pp 15−51, Wiley-VCH, Weinheim, Germany.
17. Mukai-Kuroda, Y., Fujii, R., Ko-chi, N., Sashima, T., Koyama, Y., Abe, M., Gebhard, R., van der Hoef, I., and Lugtenburg, J. (2002) Changes in molecular structure upon triplet excitation of all-trans-spheroidene in n-hexane solution and 15-cis-spheroidene bound to the photo-reaction center from Rhodobacter sphaeroides as revealed by resonance-Raman spectroscopy and normal-coordinate analysis, *J. Phys. Chem. A 106*, 3566−3579.
18. Kakitani, Y., Fujii, R., Koyama, Y., Nagae, H., Walker, L., Salter, B., and Angerhofer, A. (2006) Triplet-state conformational changes in 15-cis-spheroidene bound to the reaction center from Rhodobacter sphaeroides 2.4.1 as revealed by time-resolved EPR spectroscopy: Strengthened hypothetical mechanism of triplet-energy dissipation, *Biochemistry 45*, 2053−2062.
19. Rondonuwu, F. S., Taguchi, T., Fujii, R., Yokoyama, K., Koyama, Y., and Watanabe, Y. (2004) The energies and kinetics of triplet carotenoids in the LH2 antenna complexes as determined by phosphorescence spectroscopy, *Chem. Phys. Lett. 384*, 364−371.
20. Thurnauer, M. C., Katz, J. J., and Norris, J. R. (1975) The triplet state in bacterial photosynthesis: Possible mechanisms of the primary photo-act, *Proc. Natl. Acad. Sci. U.S.A. 72*, 3270−3274.
21. Cogdell, R. J., Monger, T. G., and Parson, W. W. (1975) Carotenoid triplet states in reaction centers from *Rhodopseudomo-*

nas sphaeroides and *Rhodospirillum rubrum*, *Biochim. Biophys. Acta 408*, 189−199.
22. Frank, H. A., Bolt, J. D., Costa, S. M. de B., and Sauer, K. (1980) Electron paramagnetic resonance detection of carotenoid triplet states, *J. Am. Chem. Soc. 102*, 4893−4898.
23. Frank, H. A., Machnicki, J., and Felber, M. (1982) Carotenoid triplet states in photosynthetic bacteria, *Photochem. Photobiol 35*, 713−718.
24. Frank, H. A., Machnicki, J., and Friesner, R. (1983) Energy transfer between the primary donor bacteriochlorophyll and carotenoids in *Rhodopseudomonas sphaeroides*, *Photochem. Photobiol. 38*, 451−455.
25. Schenck, C. C., Mathis, P., and Lutz, M. (1984) Triplet formation and triplet decay in reaction centers from the photosynthetic bacterium *Rhodopseudomonas sphaeroides*, *Photochem. Photobiol. 39*, 407−417.
26. Lous, E. J., and Hoff, A. J. (1989) Isotropic and linear dichroic triplet-minus-singlet absorbance difference spectra of two carotenoid-containing bacterial photosynthetic reaction centers in the temperature range 10−288. K. An analysis of bacteriochlorophyll-carotenoid triplet transfer, *Biochim. Biophys. Acta 974*, 88−103.
27. Frank, H. A., and Violette, C. A. (1989) Monomeric bacteriochlorophyll is required for the triplet energy transfer between the primary donor and the carotenoid in photosynthetic bacterial reaction centers, *Biochim. Biophys. Acta 976*, 222−232.
28. Frank, H. A., Chynwat, V., Posteraro, A., Hartwich, G., Simonin, I., and Scheer, H. (1996) Triplet state energy transfer between the primary donor and the carotenoid in Rhodobacter sphaeroides R-26.1 reaction centers exchanged with modified bacteriochlorophyll pigments and reconstituted with spheroidene, *Photochem. Photobiol. 64*, 823−831.
29. Angerhofer, A., Bornhäuser, F., Aust, V., Hartwich, G., and Scheer, H. (1998) Triplet energy transfer in bacterial photosynthetic reaction centres, *Biochim. Biophys. Acta 1365*, 404−420.
30. deWinter, A., and Boxer, S. G. (1999) The mechanism of triplet energy transfer from the special pair to the carotenoid in bacterial photosynthetic reaction centers, *J. Phys. Chem. B 103*, 8786−8789.
31. Monger, T. G., Cogdell, R. J., and Parson, W. W. (1976) Triplet states of bacteriochlorophyll and carotenoids in chromatophores of photosynthetic bacteria, *Biochim. Biophys. Acta 449*, 136−153.
32. Nujis, A. M., van Grondelle. R., Joppe, H. L. P., van Bochove, A. C., and Duysens, L. N. M. (1985) Singlet and triplet excited carotenoid and antenna bacteriochlorophyll of the photosynthetic purple bacterium *Rhodospirillum rubrum* as studied by picosecond absorbance difference spectroscopy, *Biochim. Biophys. Acta 810*, 94−105.
33. Papagiannakis, E., Kennis, J. T. M., van Stokkum, I. H. M., Cogdell, R. J., and van Grondelle, R. (2002) An alternative carotenoid-to-bacteriochlorophyll energy transfer pathway in photosynthetic light harvesting, *Proc. Natl. Acad. Sci. U.S.A. 99*, 6017−6022.
34. Wohlleben, W., Buckup, T., Herek, J. L., Cogdell, R. J., and Motzkus, M. (2003) Multichannel carotenoid deactivation in photosynthetic light harvesting as identified by an evolutionary target analysis, *Biophys. J. 85*, 442−450.
35. Rondonuwu, F. S., Yokoyama, K., Fujii, R., Koyama, Y., Cogdell, R. J., and Watanabe, Y. (2004) The role of the $1^1B_u^-$ state in carotenoid-to-bacteriochlorophyll singlet-energy transfer in the LH2 antenna complexes from *Rhodobacter sphaeroides* G1C, *Rhodobacter sphaeroides* 2.4.1, *Rhodospirillum molischianum* and *Rhodopseudomonas acidophila*, *Chem. Phys. Lett. 390*, 314−322.
36. Frank, H. A., Chadwick, B. W., Oh, J. J., Gust, D., Moore, T. A., Liddel, P. A., Moore, A. L., Makings, L. R., and Cogdell, R. J. (1987) Triplet-triplet energy transfer in B800−B850 light-harvesting complexes of photosynthetic bacteria and synthetic carotenoporphyrin molecules investigated by electron spin resonance, *Biochim. Biophys. Acta 892*, 253−263.
37. Farhoosh, R., Chynwat, V., Gebhard, R., Lugtenburg, J., and Frank, H. A. (1994) Triplet energy transfer between bacteriochlorophyll and carotenoids in B850 light-harvesting complexes of *Rhodobacter sphaeroides* R-26.1, *Photosynth. Res. 42*, 157−166.
38. Jirsakova, V., Reiss-Husson, F., Agalidis, I., Vrieze, J., and Hoff, A. J. (1995) Triplet states in reaction center, light-harvesting complex B875 and its spectral form B840 from *Rubrivivax gelatinosus* investigated by absorbance-detected electron spin resonance in zero magnetic field (ADMR), *Biochim. Biophys. Acta 1231*, 313−322.
39. Bittl, R., Schlodder, E., Geisenheimer, I., Lubitz, W., and Cogdell, R. J. (2001) Transient EPR and absorption studies of carotenoid triplet formation in purple bacterial antenna complexes, *J. Phys. Chem. B 105*, 5525−5535.
40. Feng, J., Wang, Q., Wu, Y.-S., Ai, X.-C., Zhang, X.-J., Huang, Y.-G., Zhang, X.-K., and Zhang, J.-P. (2004) Triplet excitation transfer between carotenoids in the LH2 complex from photosynthetic bacterium *Rhodopseudomonas palustris*, *Photosynth. Res. 82*, 83−94.
41. Alric, J. (2005) In vivo carotenoid triplet formation in response to excess light: A supramolecular photoprotection mechanism revisited, *Photosynth. Res. 83*, 335−341.
42. Fujii, R., Onaka, K., Kuki, M., Koyama, Y., and Watanabe, Y. (1998) The $2A_g^-$ energies of all-trans-neurosporene and spheroidene as determined by fluorescence spectroscopy, *Chem. Phys. Lett. 288*, 847−853.
43. Sashima, T., Koyama, Y., Yamada, T., and Hashimoto, H. (2000) The $1B_u^+$, $1B_u^-$, and $2A_g^-$ energies of crystalline lycopene, β-carotene, and mini-9-β-carotene as determined by resonance-Raman excitation profiles: Dependence of the $1B_u^-$ state energy on the conjugation length, *J. Phys. Chem. B 104*, 5011−5019.
44. Fujii, R., Ishikawa, T., Koyama, Y., Taguchi, M., Isobe, Y., Nagae, H., and Watanabe, Y. (2001) Fluorescence spectroscopy of all-*trans*-anhydrorhodovibrin and spirilloxanthin: Detection of the $1B_u^-$ fluorescence, *J. Phys. Chem. A 105*, 5348−5355.
45. Limantara, L., Sakamoto, S., Koyama, Y., and Nagae, H. (1997) Effects of nonpolar and polar solvents on the Q_x and Q_y energies of bacteriochlorophyll *a* and bacteriopheophytin *a*, *Photochem. Photobiol. 65*, 330−337.
46. Cogdell, R. J., Durant, I., Valentine, J., Lindsay, J. G., and Schmidt, K. (1983) The isolation and partial characterization of the light-harvesting pigment-protein complement of *Rhodopseudomonas acidophila*, *Biochim. Biophys. Acta 722*, 427−435.
47. Evans, M. B., Cogdell, R. J., and Britton, G. (1988) Determination of the bacteriochlorophyll:carotenoid ratios of the B890 antenna complex of *Rhodospirillum rubrum* and the B800−B850 complex of *Rhodobacter sphaeroides*, *Biochim. Biophys. Acta 935*, 292−298.
48. Zhang, J.-P., Fujii, R., Qian, P., Inaba, T., Mizoguchi, T., Koyama, Y., Onaka, K., and Watanabe, Y. (2000) Mechanism of the carotenoid-to-bacteriochlorophyll energy transfer via the S_1 state in the LH2 complexes from purple bacteria, *J. Phys. Chem. B 104*, 3683−3691.
49. Fraser, N. J., Dominy, P. J., Ücker, B., Simonin, I., Scheer, H., and Cogdell, R. J. (1999) Selective release, removal, and reconstitution of bacteriochlorophyll a molecules into the B800 sites of LH2 complexes from *Rhodopseudomonas acidophila* 10050, *Biochemistry 38*, 9684−9692.
50. Fiedor, L., Akahane, J., and Koyama, Y. (2004) Carotenoid-induced cooperative formation of bacterial photosynthetic LH1 complex, *Biochemistry 43*, 16487−16496.
51. Akahane, J., Rondonuwu, F. S., Fiedor, L., Watanabe, Y., and Koyama, Y. (2004) Dependence of singlet-energy transfer on the conjugation length of carotenoids reconstituted into the LH1 complex from *Rhodospirillum rubrum* G9, *Chem. Phys. Lett. 393*, 184−191.
52. Ohashi, N., Ko-chi, N., Kuki, M., Shimamura, T., Cogdell, R. J., and Koyama, Y. (1996) The structures of S_0 spheroidene in the light-harvesting (LH2) complex and S_0 and T_1 spheroidene in the reaction center of *Rhodobacter sphaeroides* 2.4.1 as revealed by Raman spectroscopy, *Biospectroscopy 2*, 59−69.
53. Kuki, M., Naruse, M., Kakuno, T., and Koyama, Y. (1995) Resonance Raman evidence for 15-cis to all-*trans* photoisomerization of spirilloxanthin bound to a reduced form of the reaction center of *Rhodospirillum rubrum* S1, *Photochem. Photobiol. 62*, 502−508.
54. Qian, P., Yagura, T., Koyama, Y., and Cogdell, R. J. (2000) Isolation and purification of the reaction center (RC) and the core (RC-LH1) complex from *Rhodobium marinum*: The LH1 ring of the detergent-solubilized core complex contains 32 bacteriochlorophylls, *Plant Cell Physiol. 41*, 1347−1353.
55. Fujii, R., Furuichi, K., Zhang, J.-P., Nagae, H., Hashimoto, H., and Koyama, Y. (2002) *Cis*-to-*trans* isomerization of spheroidene in the triplet state as detected by time-resolved absorption spectroscopy, *J. Phys. Chem. A 106*, 2410−2421.
56. Koyama, Y., Takii, T., Saiki, K., and Tsukida, K. (1983) Configuration of the carotenoid in the reaction centers of photosynthetic bacteria. (2) Comparison of the resonance Raman

lines of the reaction centers with those of the 14 different *cis-trans* isomers of *β*-carotene, *Photobiochem. Photobiophys. 5*, 139−150.
57. Wilson, G. S. (1978) Determination of oxidation-reduction potentials, *Methods Enzymol. 54*, 396−410.
58. Leigh, J. S., Jr., and Dutton, L. (1974) Reaction center bacteriochlorophyll triplet states: Redox potential dependence and kinetics, *Biochim. Biophys. Acta 357*, 67−77.
59. Jungas, C., Ranck, J.-L., Rigaud, J.-L., Joliot, P., and Verméglio, A. (1999) Supramolecular organization of the photosynthetic apparatus of *Rhodobacter sphaeroides*, *EMBO J. 18*, 534−542.
60. Andersson, P. O., Gillbro, T., Ferguson, L., and Cogdell, R. J. (1991) Absorption spectral shifts of carotenoids related to medium polarizability, *Photochem. Photobiol. 54*, 353−360.
61. Kuki, M., Nagae, H., Cogdell, R. J., Shimada, K., and Koyama, Y. (1994) Solvent effect on spheroidene in nonpolar and polar solutions and the environment of spheroidene in the light-harvesting complexes of *Rhodobacter sphaeroides* 2.4.1 as revealed by the energy of the $^1A_g^- \rightarrow {}^1B_u^+$ absorption and the frequencies of the vibronically coupled C=C stretching Raman lines in the $^1A_g^-$ and $2^1A_g^-$ states, *Photochem. Photobiol. 59*, 116−124.
62. Englman, R., and Jortner, J. (1970) The energy gap law for radiationless transitions in large molecules, *Mol. Phys. 18*, 145−164.
63. Kuki, M., Koyama, Y., and Nagae, H. (1991) Triplet-sensitized and thermal isomerization of all-*trans*, 7-*cis*, 9-*cis*, 13-*cis*, and 15-*cis* isomers of *β*-carotene: Configurational dependence of the quantum yield of isomerization via the T_1 state, *J. Phys. Chem. 95*, 7171−7180.
64. Koyama, Y., Kanaji, M., Shimamura, T. (1988) Configurations of neurosporene isomers isolated from the reaction center and the light-harvesting complex of *Rhodobacter sphaeroides* G1C. A resonance Raman, electronic absorption, and ^{1}H-NMR study, *Photochem. Photobiol. 48*, 107−114.
65. Koyama, Y., Takatsuka, I., Kanaji, M., Tomimoto, K., Kito, M., Shimamura, T., Yamashita, J., Saiki, K., and Tsukida, K. (1990) Configurations of carotenoids in the reaction center and the light-harvesting complex of *Rhodospirillum rubrum*. Natural selection of carotenoid configurations by pigment protein complexes, *Photochem. Photobiol. 51*, 119−128.
66. Rondonuwu, F. S., Watanabe, Y., Fujii, R., and Koyama, Y. (2003) A first detection of singlet to triplet conversion from the $1^1B_u^-$ to the 1^3A_g state and triplet internal conversion from the 1^3A_g to the 1^3B_u state in carotenoids: Dependence on the conjugation length, *Chem. Phys. Lett. 376*, 292−301.
67. Takiff, L., and Boxer, S. G. (1988) Phosphorescence spectra of bacteriochlorophylls, *J. Am. Chem. Soc. 110*, 4425−4426.
68. Takiff, L., and Boxer, S. G. (1988) Phosphorescence from the primary electron donor in *Rhodobacter sphaeroides* and *Rhodopseudomonas viridis* reaction centers, *Biochim. Biophys. Acta 932*, 325−334.

BI062237Z